Master's thesis

2019

Peter Martinius Stige

NTNU
Norwegian University of
Science and Technology
Faculty of Information Technology and Electrical
Engineering
Department of Engineering Cybernetics

Peter Martinius Stige

Modelling and Implementation of Glycemic Response Calculator

June 2019

NTNU
Norwegian University of
Science and Technology

NTNU
Norwegian University of
Science and Technology

NTNU
Norwegian University of
Science and Technology

Modelling and Implementation of Glycemic Response Calculator

Cybernetics and Robotics
Submission date: June 2019
Supervisor: Anders Lyngvi Fougner
Co-supervisor: Steinar Sælid

Norwegian University of Science and Technology
Department of Engineering Cybernetics

NTNU
Norges teknisk-naturvitenskapelige universitet

Fakultet for informasjonsteknologi, og elektroteknikk
Institutt for teknisk kybernetikk

MASTEROPPGAVE

Kandidatens navn: Peter Martinius Stige

Fag: Teknisk kybernetikk, masteroppgave (TTK4900)

Oppgavens tittel (norsk): **Modellering og realisering av glykemisk responskalkulator**

Oppgavens tittel (engelsk): **Modelling and implementation of glycemic response calculator**

Oppgavens tekst:

Prediktor Medical AS is a company developing a wearable non-invasive continuous glucose monitor (CGM) called BioMKR. Related to this, they are working on modelling, prediction and control of plasma glucose in patients with diabetes mellitus type 1 and 2.

The purpose of this MSc thesis is the following:

- To be able to identifiy the parameters of a metabolism model based on the measurements of a CGM over a time period.
- Use this model as a predictive tool for users to do «what if»-analyses, as well as to propose insulin bolus amounts for planned meals.

This thesis includes the following tasks:

1. Give a summary of the existing theories and methods for explaining and modelling the glycemic response after consuming different food products. Look especially at the article:

   Rozendaal, Yvonne J., et al. "*Model-Based analysis of postprandial glycemic response dynamics for different types of food.*" Clinical Nutrition Experimental 19 (2018): 32-45.

   This reference bases its work on published data that might be used in this thesis.

2. A model like this requires meal data as input. A potential use for a person with diabetes requires the model to be easy to use. A possible input method could be to use the camera of a smartphone, together with an image analysis tool (classification), to estimate meal parameters. Give a summary of work reported in this field of research, and take a look at:

   Domhardt, Michael, et al. "*Training of carbohydrate estimation for people with diabetes using mobile augmented reality.*" Journal of diabetes science and technology 9.3 (2015): 516-524.

   Discuss these methods and whether they can be used to get input for a glycemic model.

3. Implement a glycemic response calculator based on a metabolism model. The implementation is based on a model with a complexity fit for purpose. Glycemic predictability and necessary identifiability must be emphasized. The latter because a possible use of the of this could be for identification of glycemic parameters based on real time data from a CGM.

Oppgaven gitt: 7. januar 2019

Besvarelsen leveres innen: 3. juni 2019

Utført ved Institutt for teknisk kybernetikk

Veileder: Anders Lyngvi Fougner
Biveileder: Steinar Sælid, Prediktor Medical AS

Trondheim, 10. desember 2018

Abstract

For people with diabetes mellitus, it is crucial to keep the plasma glucose concentration levels in inside the recommended range after meals. Many do this by counting carbohydrates manually, and deciding the insulin bolus thereafter. To help with this, a glucose response calculator which takes more than the amount of carbohydrates into consideration would be a useful aid.

In this project, the use of a glycemic model as the foundation of a glycemic response calculator have been studied.

A summary of theories and methods to explain and model glucose responses after meal intake have been presented. Different research in the area of meal parameter estimation is described, with emphasis on using a smartphone camera with image classification algorithms to estimate.

Glucose response studies described in Rozendaal et al. [1] was collected and put into a dataset, together with additional macronutrient information about the meals. Also, two study subjects used CGMs to record plasma glucose measurements in their daily lifes, while they also wrote down what they ate, and when. The data gathered were analysed using PLSR, to find the correlations between meal parameters and glucose responses. The PLSR analysis showed some correlation between the macronutrients (fat, protein and fiber) and the glucose response.

Two lower order glycemic models, namely *The identifiable virtual patient model* (IVP) and *The subcutaneous oral glucose minimal model* (SOGMM), was altered in three different ways, to take into account the amount of fat, protein and fiber in the meals when predicting glucose responses. The meal input and glucose response data was used in parameter estimation algorithms, to try and predict meal responses. The results were compared to the results of predictions using the unaltered models, without fat, protein and fiber as input. The largest model, SOGMM, obtained the best prediction results overall. The inverse correlations found between glucose response and fat, protein and fiber in the PLSR analysis, were not reproduced in the glycemic model predictions. In general, the models not taking fat, protein and fiber into account did better than the models that did.

Sammendrag

For personer med diabetes mellitus er det avgjørende å holde blodsukkernivået innenfor det anbefalte området etter måltider. Mange gjør dette ved selv å telle karbohydrater, og deretter bestemme mengden insulin som skal settes. En glykemisk responskalkulator som tar mer enn bare karbohydrater med i betraktningen ville vært et nyttig hjelpemiddel for dette.

I dette prosjektet har bruken av en glykemisk model som grunnlag for en glykemisk responskalkulator blitt undersøkt.

Et sammendrag av teorier og metoder for å forklare og modellere blodsukkerrespons etter måltider har blitt presentert. Forskjellig arbeid på feltet som omhandler estimering av måltidsparametere er beskrevet, med vekt på å bruke et mobilkamera sammen med et bildeanalyseringsprogram for å estimere.

Blodsukkerrespons-studier brukt i Rozendaal et al. [1] ble samlet og puttet i et datasett, sammen med ytterligere info om næringsstoffer i måltidene. To forsøkspersoner målte også blodsukkeret sitt over to uker, ved bruk av CGM, mens de samtidig noterte hva de spiste, og når. Den samlede dataen ble analysert ved bruk av PLSR, for å finne korrelasjoner mellom måltidsparametere og glykemisk respons. PLSR-analysen viste noe korrelasjon mellom makronæringsstoffene (fett, protein og fiber) og blodsukkerrespons.

To lavere ordens glykemiske modeller, kalt *The identifiable virtual patient model* (IVP) og *The subcutaneous oral glucose minimal model* (SOGMM), ble endret på tre forskjellige måter, for å kunne ta hensyn til mengden fett, protein og fiber i måltidene, for å predikere blodsukkerresponser. Måltidsparameterene og blodsukkerresponsene ble brukt i algoritmer for modellparameterestimering, for å prøve å forutse måltidsresponser. Resultatene ble sammenliknet med resultatene fra prediksjoner gjort med de originale modellene, som ikke tar hensyn til fett, protein og fiber. Den største modellen, SOGMM, oppnådde de beste prediksjonsresultatene totalt sett. Den inverse korrelasjonen funnet mellom blodsukkerrespons og fett, protein og fiber i PLSR-analysen, ble ikke reprodusert i prediksjonene utført av de glykemiske modellene. Generelt klarte modellene som ikke tok hensyn til fett, protein og fiber å predikere bedre enn modellene som gjorde det.

Preface

This master's thesis covers my master's project at the Cybernetics and Robotics programme at the Norwegian University of Science and Technology. The project was carried out during the spring semester of 2019, and is a continuation of the work from my term project "Implementation of a Metabolism Model for Insulin/Glucose Dynamics" autumn 2018. This study is intended to be a contribution to the rapid development in the study of diabetes and glucose control. The supervisor of my thesis was Anders Lyngvi Fougner, and my supervisor was Steinar Sælid.

The university and Predictor provided me tools necessary to carry out the project. A list of information, apparatus and software used in the project follows:

- Two FreeStyle Libre sensors and one FreeStyle Libre reader was provided by Prediktor. The continuous glucose data was imported to a computer using the FreeStyle Libre Software, downloaded from their website.
- Prediktor lent out a Macbook Air for me to use in my work. This was done in the hope that I would be able to continue my work on the iPhone application, GlucoPredMobile, on which was started summer 2018. Unfortunately, there was no time left to do this.
- Unscrambler X was used for the PLSR analysis, provided by NTNU's programfarm.
- Matlab was used for all model implementation and model analysis, with the Matlab license provided by NTNU.
- Matlab code from my term project autumn 2018 on identifiability of the GlucoPred metabolism model [2] was used and built upon. This includes code implementing parameter sensitivity analysis for a simulation model and model parameter estimation methods.
- Some paragraphs from the theory section of the term project are cited in the theory section of this thesis. It is mentioned at the start of the given section or paragraph, if it is cited from the term project.

Acknowledgements

I want to thank the following people:

Anders Lyngvi Fougner for being my great supervisor at NTNU, always helping and challenging me to do my best.

Steinar Sælid for being my enthusiastic co-supervisor from Prediktor, very knowledgeable and with an answer to every question.

Odd Martin Staal for giving me a good introduction to metabolic modelling and model analysis last summer.

APT (Artificial Pancreas Trondheim) for letting me (and the other M.Sc. students) join your meetings, and thereby being a source of feedback and inspiration for the project.

My girlfriend for always being there when I need it, supporting and motivating me through the semester.

Contents

List of Figures

List of Tables

Nomenclature

aCHO	Available Carbohydrates
ANN	Artificial neural network
CNN	Convolutional neural network
E-DES	Eindhoven Diabetes Education Simulator
EV	Explained Variance
GI	Glycemic index
GL	Glycemic load
IVP	Identifiable Virtual Patient model
PLSR	Partial Least Squares Regression
PPGR	Postprandial glucose response
RF	Random forests
RSV	Right Singular Vector
SIFT	Scale-invariant feature transform
SOGMM	Subcutaneous Oral Glucose Minimal Model
SVM	Support-vector machine

1 Introduction

Diabetes Mellitus (DM) is a disease in which defects in insulin action (Diabetes Mellitus 2) or insulin secretion (Diabetes Mellitus 1) can lead to hyperglycemia. In the world today, 425 million adults have diabetes, where 212 million of those are undiagnosed [3]. Precise insulin administration is very important for people with Diabetes Mellitus to control their glucose levels, especially right after meals. Today, the dosage of exogenous insulin is mainly done manually, with patients injecting it subcutaneously, either with an insulin pen/syringe, or via an insulin pump.

Different food compositions can lead to different postprandial glucose responses (PPGR). There are many factors that contribute to this response. For one, meal macronutrients like carbohydrates, fat, protein and fiber, and other meal characteristics, affect the PPGR. Another very important factor is the patient's physical properties, and how the body responds to different meals. These physical properties are not constant, but will have a natural variation during and between days [4, 5]. Also, different patients can (and will, in most cases) show small or large differences in glucose response to the same meal [6]. This is why it is important to have data from the subject in question when trying to predict its glucose response after a meal. All of this makes for a difficult task to predict the PPGR of a patient.

A crucial part of blood glucose control for a DM1 or DM2 patient is to estimate the amount of carbohydrates they eat, because this is largely how the insulin bolus size is determined. Studies show that for most people, manual carbohydrate amount estimation is very hard to do precisely, and that patients might have a tendency to underestimate the amount of carbohydrates in their meal [7, 8]. Therefore several carbohydrate estimation tools have arrived, many based on the use of a mobile phone camera and image classification algorithms. The patient takes one or two pictures or just points the camera towards the meal, and the estimation algorithm does the rest. A tool able to estimate carbohydrates in a meal will easily be able to estimate other macronutrients in the same meal as well. These macronutrient could be helpful in the task of predicting the glucose response, as mentioned above.

Combining solutions for these two problems, that is, knowing which type of meals which lead to what PPGR and estimating the meal composition precisely, could be a very helpful tool for diabetic patients in their daily life.

This thesis will start with some basic theory, presented in section 2, important for understanding the rest of the article. The aim of the study is described in section 3. Section 4 contains a literature study, presented in two parts. First, a summary of the existing theories and methods to model and explain PPGR is presented in section 4.1. This will focus on meal characteristics and meal parameters which have an effect on the PPGR, and how they affect it. It will also focus on different glycemic simulation models that can be used to simulate

and predict PPGR, in addition to some of the biological explanations behind them, what is included in the models and what is not included. Then, different methods to estimate meal parameters using a smartphone camera is described in section 4.2. The focus in this part will be on the different ways this is done in literature and research, and then especially meal classification and meal size estimation.

The methods and approaches used in this project will be presented in section 5, before the results are presented in section 6. In these sections, data from healthy subjects gathered in Rozendaal et al. [1], from multiple studies, will be used in a correlation analysis between meal macronutrients and PPGR. Two lower order glycemic models will be altered so that they take meal macronutrient into account. Furthermore, glucose measurements gathered from two healthy subjects will be presented, analysed with PLSR and used to test the precision of PPGR prediction with the two aforementioned glycemic models. The results are discussed in section 7, and conclusions presented in section 8.

2 Theory

2.1 Partial least squares regression

Partial least squares regression (PLSR) PLSR is a statistical method for multivariate regression. It performs prediction from the predicting variables X to responses Y. The underlying model equations for PLSR is:

$$X = TP^T + E \tag{2.1}$$

$$Y = UQ^T + F \tag{2.2}$$

T and U are the mapping of X and Y onto the latent variables. T and U are called the scores for X and Y. P and Q are called the loadings for X and Y.

A regression model is built, based on a transition from the original predicting variables X to a smaller number of latent variables. The regression model can be built using algorithms like NIPALS, kernel PLS or others [9], and the aim is for the latent variables to explain the response variables as best as possible.

PLSR factors The factors of the regression model are a new variable space rotated from the input variables X, to explain as much of the responses Y as possible. The first factor points in the direction in the X space which explains as much of Y as possible. When the direction of the first factor is excluded from X, X holds one less dimension. Then the same procedure is carried out again on the new X. The second factor explains as much of the rest of the variance in Y as possible, and so on.

Loadings The loadings describe where in this new factor space the inputs X are positioned. The two first factors have the highest explanation of Y. If an input variable has a low absolute value for both of these factors, it will most likely have a low impact on the prediction of Y.

The "Correlation Loadings" plot shows, like in figure 6.2, which of the input variables that are important, and which are not. The dots represent input variables X (blue dots) or output variables Y (red dots). The further away from the center of the plot an input variable is positioned, the more important it is for the PLSR model and the prediction of future outputs. The inputs inside the inner circle will not be very important in the predictions, while the inputs outside it will be important. If an input is positioned on the outer circle, this one is absolutely crucial for the PLSR model.

Explained variance The explained variance (EV) describes what percentage of the variance in the responses Y that can be explained by the input variables

X. The EV plot shows, like in figure 6.1, the EV percentage against the number of factors included in the prediction. For some models, only one or two of the input variables will be important. If this is the case, the EV plot will increase a lot from factor-0 to factor-1. From factor-1 and onwards it will not raise as much, because the rest of the data does not contain information that is valuable in the PLSR model and its predictions of Y. If, on the other hand, all input variables are equally important, the EV will raise much slower from factor to factor, and the last factor will typically have the highest EV in the plot.

Cross validation Cross validation is a method that can be used to validate model prediction results. A total sample set is divided into a training/calibration set on which a model is trained, and a validation set on which the model prediction is tested. This ensures that each sample are represented in the validation set at least once.

In a dataset with N samples, a k-fold cross validation includes N/k samples in the validation set for each of the k training rounds. Random k-fold cross validation means that for each round, the validation set is picked randomly from the total set of samples.

Leave-one-out cross validation means to let the validation set consist of only one sample each training round, and the training/calibration set consists of the rest of the samples.

2.2 Metabolism models

The last two paragraphs of this part is cited from Stige [2].

A metabolism model describes the dynamics between glucose and insulin in the human body. It is a collection of ordinary differential equations, interacting with each other to simulate the behaviour of the metabolism in the body.

There are a variety of different metabolism models. They have different complexity levels, include different dynamics in their equations and are used differently dependent on what they are modelling. One example is the Bergman minimal model. It consists of three state variables, plasma glucose concentration $G(t)$, plasma insulin concentration $I(t)$ and insulin in remote compartment $X(t)$ [10]. It only models how glucose and insulin is injected into the blood, so for it to work as a complete glucose-insulin metabolism model, several things needs to be added, including for example a model of the digestive system and realistic exogenous insulin injection. This is one of the simplest models there is. A more complex model is the UVa/Padova type 1 diabetes simulator [11, 12]. This model has 18 state variables, and is much more complex than the minimal model. This model is therefore used for more complex tasks than the minimal model.

A metabolism model contains a number of parameters representing different phenomena in the body. One example is the parameter S_i, usually representing insulin sensitivity in many metabolism models for glucose and insulin dynamics. These parameters have to be identified for the model to be able to represent a person realistically.

2.3 Identifiability

This part are cited from Stige [2].

Observability is a property a system can have which implies that the values of the state variables can be determined from the output of the system. This is a desired property of a system because unknown state variables can make control of the system harder.

Identifiability considers whether the parameters in a system of differential equations can be uniquely determined from the input and the output of the system. If this is the case, the system is called identifiable. If a system is non-observable, it implies that it is also non-identifiable. Many types of identifiability have been introduced ([13, 14]), but practical identifiability is the only concept used here.

A practical identifiability analysis looks at the identifiability when we do not have perfect and noise-free measurements. Lack of practical identifiability can be caused by several things. One of them is that the model structure makes it not structurally identifiable, and therefore also not practically identifiable. Even though a parameter set for a model is structurally identifiable, it is not always identifiable in practice, and this may be caused by two things. The first is that the model is not sensitive to one or more parameters in the set. The other is that two or more parameters correlate, that is, their contribution to the model output cannot be distinguished from each other [15]. A kind of practical identifiability analysis is sensitivity analysis, described in section 2.4.

2.4 Sensitivity analysis

This part is cited from Stige [2].

Sensitivity analysis is a kind of practical identifiability analysis and a way to obtain information about how much the different model parameters influences the model output. The sensitivity of a parameter can be seen as

$$\mathbf{S}_{p_i} = \frac{\partial \mathbf{y}}{\partial p_i}$$

That is, the derivative of the output $\mathbf{y}$ with respect to the parameter p_i. This only gives the sensitivity at one time instant. To get the parameter sensitivity over the course of a simulation, a system of ODEs must be developed, based on

the original system equations, like in Stigter et al. [16]. These equations will model the sensitivity dynamics between the model and its parameters, and can be given as:

$$\dot{\mathbf{x}}_p(t) = \frac{\partial \mathbf{f}}{\partial \mathbf{x}} \mathbf{x}_p(t) + \frac{\partial \mathbf{f}}{\partial \mathbf{p}} \tag{2.3}$$

$$\dot{\mathbf{y}}_p(t) = \frac{\partial \mathbf{h}}{\partial \mathbf{x}} \mathbf{x}_p \tag{2.4}$$

Here $\mathbf{f}$ is the vector of the original model equation expressions, $\mathbf{h}$ is the output equations, $\mathbf{x}$ is the state vector and $\mathbf{p}$ is the parameter vector. $\mathbf{y}_p(t)$ is a vector with the parameter sensitivity at time t. These vectors can be put together in a sensitivity matrix $\mathbf{S}$. In this matrix each row is the sensitivity vector of one output at one time instant. Each column corresponds to the sensitivity for a single parameter over the course of the simulation. This way, by plotting one column over the simulation time, we can observe in which parts of the simulation a parameter has high sensitivity, and for which it has lower or no sensitivity.

2.5 Model parameter estimation

2.5.1 Objective function for parameter estimation

This part is cited from Stige [2].

One way objective function minimization can be done is to use the model and vary the parameters so that a simulation of it is fitted to the desired output measurement. The two sided desirability function [17, 18] can be used as an objective function for this purpose. This function is on the form

$$d_{tot}(\mathbf{x}, \mathbf{y}) = -d_y \prod_{i=1}^{n_{par}} d_{x,i} \tag{2.5}$$

where d_y is given by

$$d_y = d(y, n_y) \tag{2.6}$$

$$y = \sqrt{\frac{1}{n_{sim}} \sum_{i=1}^{n_{sim}} (y_{sim} - y_{ref})^2} \tag{2.7}$$

$d_{x,i}$ is given by

$$d_{x,i} = d(x_i, n_x) \tag{2.8}$$

and $d(x, n)$ is given by

$$d(x, n) = \exp\left[-(\tilde{x}(x))^n\right] \tag{2.9}$$

$$\tilde{x}(x) = \frac{2x - (x_{max} + x_{min})}{x_{max} - x_{min}} \tag{2.10}$$

Here x_{min} and x_{max} are the minimum and maximum values of the parameters estimated, given for all parameters in Appendix A.1 and Appendix A.2.

d_y is a measure of the difference between $\mathbf{y}_{sim}$ and $\mathbf{y}_{ref}$. $\mathbf{y}_{sim}$ is the glucose values of a simulation with parameter values from $\mathbf{x}$, and $\mathbf{y}_{ref}$ the simulated measurement glucose values that we want to obtain with the model parameter estimation. n_{sim} is the number of time steps in the simulation.

$d_{x,i}$ gives a value near 1 if the parameter value is in the desired region, and lower values the further away it is from that region. The higher n is, the wider this region becomes, so that parameters moving away from the middle does not decrease as fast. When $n \to \infty$, the function will approach the boxcar function. The boxcar function is a function which evaluates to zero outside the region $[x_{min}, x_{max}]$, and 1 inside it.

2.5.2 Downhill simplex method (Nelder-Mead)

This part is cited from Stige [2].

The downhill simplex method is a derivative-free method for solving non-linear optimization problems. Instead of derivatives it uses a simplex in the parameter space to narrow the search space until it finds a minimum point of the function. A simplex is a polytope with n+1 vertices, in n dimensions. Each vertex of the simplex is a set of parameter values in the parameter space, with a corresponding objective function value.

The fundamental idea behind the simplex method is that the vertex in the current simplex with the "worst" objective function value is mirrored through the line between the two vertices with the "best" objective function values. Then the objective function is evaluated at this new point. If it is good, it replaces the worst vertex in the simplex. If it is not so good, a new point closer to the worst point along the mirroring line is evaluated. This way, the simplex will always try to move towards the parts of the parameter space with better objective function values.

2.6 The digestive system

In the following, the digestive system will be described, with emphasis on the parts that affects the plasma glucose concentration. Information for this part is from Nicolaysen and Holck 2013 [19].

Mastication The food digestion starts already in the mouth/oral cavity. Here the food is mechanically divided into smaller parts by chewing and prepared to enter the stomach and guts. The spit/saliva produced in the oral cavity is important to satisfy digestion and absorption of nutrients later on.

Stomach decomposition When food is swallowed it is led from the mouth through the esophagus to the stomach. The swallowing triggers wave-like muscle contractions in the esophagus to push the food downwards. The production of gastric acid in the stomach is increased when the food bolus is getting closer to the stomach, and is further increased when the food has entered the stomach. The gastric acid contains hydrochloric acid, which activates enzymes which breaks down different components of the food. The food is led from the upper part to the lower part of the stomach by muscle contractions in the wall of the stomach.

Gastric emptying When the processed food bolus approaches the bottom of the stomach, the pylorus will open and let the food be emptied to the duodenum. This gastric emptying is controlled by many factors, like the amount of food and the food form (solid, liquid). When the food is passing through the duodenum, different hormones are secreted. Some of these hormones will inhibit the gastric emptying if the food contains much fat, or if it has low pH value. This will be done because fat is digested relatively slowly i the duodenum, so small amounts should enter at the time. Also, the duodenum is sensitive to low pH values, so the gastric acid needs to be neutralized by bicarbonate secreted from pancreas.

Gut absorption In the small intestine, most of the nutrients are absorbed. The mucous membrane of the intestine has a large surface, because it is folded with many small intestinal villi on it. Also here the food is kneaded and brought forward by wave-like muscle contractions in the intestine. This is important to get the food in contact with as much as the surface as possible, so the nutrients are absorbed.

2.7 Plasma glucose control

2.7.1 Healthy subjects

Healthy people with a working pancreas and normal insulin sensitivity will have a good regulation of the plasma glucose concentration. This is because hormones such as insulin, glucagon and adrenalin controls it by lowering (insulin) and increasing (glucagon and adrenalin) the plasma glucose as needed.

Both insulin and glucagon are produced in the pancreas, in the β- and α-cells respectively. This is done through control mechanism based on, among other things, the plasma glucose concentration level and its rate of change. Insulin helps lowering the plasma glucose by letting it be turned into glycogen in the liver and in the muscles. The glycogen in the muscles can only be utilized as energy by the muscle itself. The liver glycogen on the other hand, works as a glycogen storage, and can be turned into glucose again through the supply of glucagon. This way, glucagon helps increasing the plasma glucose when that is needed.

2.7.2 Diabetes mellitus subjects

For a person with diabetes mellitus 1, insulin will not be secreted from the β-cells in pancreas, and therefore the plasma glucose will increase uncontrollably after a meal, if external insulin is not injected. A person with diabetes mellitus 2 will not normally be dependent on external insulin. The β-cells work, but the insulin is not utilized as well as for a healthy person, because the insulin sensitivity is low. A person with diabetes mellitus 2 who do not control their plasma glucose very well, might also be dependent on external insulin.

External insulin boluses are normally injected into the subcutaneous skin-layer. They can be slow working basal doses, intended to work all day, or fast-working boluses associated with meals. From the subcutaneous skin layer, the insulin is slowly transferred to plasma over time, with the transfer rate dependent on the type of insulin injected.

3 Aim of the study

The aim of this study is to give a contribution to the work of modelling, prediction and control of plasma glucose for DM1 and DM2 patients. Most insulin bolus calculators only considers the amount of carbohydrates of the meal that is eaten. By investigating how the macronutrients of meals affect the postprandial glucose responses for healthy subjects, this can more easily be investigated for DM1 and DM2 subjects later. The project is in cooperation with Prediktor Medical AS, where the development of a non-invasive continuous glucose monitor is in progress.

This project will present:

- A presentation of existing theories for explaining postprandial glycemic response to meals, and methods for meal estimation and classification using a smartphone camera.
- Analysis of the correlation between meal macronutrient content and glucose responses.
- Analysis of two lower order glycemic models, and their prediction results, based on meal macronutrient input.

4 Literature study

4.1 Explaining postprandial glycemic responses

To predict the PPGR of an individual is not an easy task, because so many factors come in to play. In this section, different efforts to explain and model the PPGR are presented, together with the most important parameters which can have an effect on, and thus help predict, the PPGR.

4.1.1 Meal parameters

A meal can be described by many different parameters. The most important one in terms of managing the plasma glucose and insulin dosing for diabetic patients is the amount of available carbohydrates in the meal. This means the total amount of carbohydrates minus the amount of dietary fiber, which can not be digested and transformed to glucose in plasma. Another parameter which can describe the meal is the glycemic index (GI), which is a description of the expected area under the curve in the PPGR of a meal. Also other macronutrients such as fat, protein and dietary fiber can have an impact on the PPGR, but in the opposite way, since none of these three are turned into plasma glucose during the digestion process. The following will present these, and their properties as predictors of PPGR.

Carbohydrates The amount of available carbohydrates (aCHO) in a meal is a key factor for the PPGR, since it is the carbohydrates that are turned into plasma glucose during digestion. Therefore, diabetic patients have to be careful when managing their meals in terms of the amount of available carbohydrates. A simplified view is that eating too much carbohydrates compared to the injected insulin bolus can lead to hyperglycemia, but eating too little can lead to hypoglycemia.

Carbohydrates come in three different forms. Rapidly digested mono- and disaccharides called sugars, more slowly digested polysaccharides called starch, and non-digestable carbohydrates called fiber [20]. Since different carbohydrates will not be digested at equal rates, the PPGR will be different when you eat 50 grams of sugar than if you eat a whole grain bread with 50 grams of aCHO. This is one of the reasons that aCHO alone is not a sufficient parameter to use to predict the PPGR accurately.

Glycemic index and glycemic load The glycemic index (GI) [21, 22] is a parameter which describes a meal's plasma glucose response after intake. It is determined by letting a group of subjects (preferably ten or more) eat the food/meal and then measure the PPGR. The relative area under the glucose

curve compared to the area under the curve for an oral glucose tolerance test (OGTT) determines the GI value. This is a value between 0 and 100, where 0 describes no area under the curve and 100 describes an equal area under the curve as for an OGTT. In 2013, international carbohydrate experts held a scientific summit on glycemic index and glycemic load, and the result was a consensus recognizing the relevance of glycemic index and glycemic load in the prevention and management of diabetes [23]. Lan-Pidhainy et al. [24] investigated the clinical utility of GI based on whether it is the same for healthy and DM2 subjects. They concluded that GI is a valid property for foods, because it was similar for both healthy and DM2 subjects.

Liu et al. 2012 [25] showed that when reducing the glycemic index and/or the carbohydrate content of a meal, the PPGR is lowered. This is an expected result, since the GI describes the area under the curve of the PPGR, and carbohydrates are digested into plasma glucose. This further indicates that the GI is a parameter one should consider when trying to predict the PPGR.

It has also been shown that the glycemic index is a stronger predictor of the PPGR than only carbohydrate content alone [26]. Another study, from Fabricatore et al. [27], showed that between carbohydrate content, GI, fiber and other macronutrients, GI was the strongest independent predictor of glycemic area under curve, glycemic mean values, and euglycemic and hyperglycemic range values.

Another food parameter based on area under curve is the glycemic load (GL) [22]. GL is simply the GI multiplied with the amount of carbohydrates. This way, two meals with the same GI, but where one of them contains a higher amount of carbohydrates, this meal will have a higher GL than the other meal. The results in Bao et al. [28] shows that GL is a better and more consistent predictor of PPGR than only the amount of available carbohydrates alone. Also Brand-Miller et al. [29] supported the glycemic load as a consistent predictor of glycemic response.

The problem with using GI and GL for predicting PPGR is the following. First of all, the GI and GL values for each food/meal will most likely never be 100% correct. Even though Lan-Pidhainy et al. [24] found similar values across subject groups, the GI is based on measurements of the plasma glucose concentrations in real humans, which means that the values are dependent on the subject group and also day-to-day variations [30]. This will have an effect, even though the GI values are determined for a study group of at least 10 subjects.

Second, the GI does not measure how fast the carbohydrates are turned into plasma glucose, it only describes the area under the curve of the GGPR. This means that a meal that gives a really fast response, almost like a spike, can have the same GI as a meal that is digested much slower. This slower meal will have a lower maximum plasma glucose concentration value, but the response will last much longer. This highlights some of the limitations in the GI and GL

as predictors of PPGR.

Fat, protein and fiber Three meal parameters that does not affect the plasma glucose directly are the amount of fat, protein and fiber in the meal. They do, however, affect the plasma glucose by taking up space in the stomach. Therefore, if a meal contains much fat, protein and/or fiber, it will likely take longer before the carbohydrates are released into the duodenum. Shukla et al. [31] reported that to eat food containing much fat and protein before a carbohydrate-rich meal will give a lowered PPGR compared to eating the carbohydrate-rich meal first.

Fat is digested into fatty acids, and does not increase the plasma glucose when eaten. On the contrary, meals containing much fat delays the uptake of carbohydrates, and the PPGR may turn out slower and/or lower than for another meal containing the same amount of carbohydrates. This is also partly because of the dynamic described in section 2.6, that more fatty food in the duodenum slows down the gastric emptying.

Henry et al. [32] showed that different types of oils or butter eaten together with white bread gave a significant decrease in both peak plasma glucose and the area under curve, compared to white bread alone. Owen et al. [33] showed the same, but only for non-hydrogenated-fat from margarine. Also Lodefalk et al. [34] showed that the area under the curve of the plasma glucose after a meal was reduced with the addition of dietary fat, to meals with the same amount of carbohydrates and protein, for DM1 patients. It was also shown that the gastric emptying was slower for the high-fat meal than for the low-fat one. Also Frost et al. [35] also showed delay of gastric emptying, when adding fat to a pasta meal. They also showed a decrease in plasma glucose when fat was added. Wolever et al. [36] found that for healthy subjects fat reduced the PPGR only after 15 and 30 minutes. Also for DM1 subjects, fat delayed the PPGR, but not significantly. Therefore, fat could be important to consider when trying to predict the PPGR.

Protein is digested into amino acids, and it does not increase the plasma glucose when eaten either. Nuttall et al. [37] showed that, for at least some DM2 patients, 50 g protein given together with 50 g glucose lowers the glucose response. Karamanlis et al. [38] showed that protein lowers PPGR to oral glucose, and increases the gastric half-emptying time. Also Gunnerud et al. [39] found that meals based on milk/milk protein gave lowered glycemic responses compared to white wheat bread with the same amount of carbohydrates. This effect appeared to originate from the protein fraction of the meals. Therefore it is reason to believe that protein has the same effect on the PPGR as fat does.

Moghaddam et al. [40] reported that both protein and fat reduced the AUC and peak rise value of the plasma glucose concentration when consumed together with 50 g of glucose. They also reported that the effects of fat and pro-

tein were independent, but that the effects of protein were 2-3 times larger than the effects of fat.

Neu et al. [41] showed that when DM1 adolescents ate a standard meal (SM) and a fat-protein-rich meal (FPRM) with the same amount of carbohydrates, in the evening, the plasma glucose was higher for the FPRM than for the SM after 12 hours. This shows that for DM1 patients, it is not only the immediate PPGR that should be considered, but also the delayed response, because of fat and protein.

Fiber is a type of carbohydrate, but it is not digestible. This means that it is not digested into glucose in the body, and does not increase the plasma glucose concentration when eaten. It is shown that high-fiber cereal eaten 75 minutes before a meal, lowers the PPGR to the meal compared to a low-fiber cereal or white bread [42]. Jenkins et al. [43] showed that adding different types types of fibers (12 grams) to OGTTs reduced the glucose responses significantly at one or more points during the tests. Holt et al. [44] got similar results, but also found that the lowered glucose response could be caused by the fiber's delay of gastric emptying. Therefore, it might be the case that fiber has the same effect on the PPGR as fat and protein.

4.1.2 Modelling of PPRG

Presented here is a group of metabolism models, with emphasis on how they have modelled the digestive system, glucose absorption and insulin action. None of the presented models have meal fat, protein or fiber as input in the first place.

Modelling of the interaction between insulin and glucose in the body must be done differently for a healthy, DM1 or DM2 subject. In a healthy subject, eating a meal and/or raising the plasma glucose will lead to insulin secretion in the pancreatic β-cells. Therefore, an expression representing the pancreatic insulin secretion based on the plasma glucose should be included in a healthy subject model. Many models solve this by including an expression including both the plasma glucose and its positive rate of change [12, 2], in addition to a basal insulin secretion rate. Other criteria is often also included, such as a plasma glucose threshold for which the insulin secretion based on the plasma glucose should work.

A person with DM1 will not produce insulin in the pancreas, because the β-cells do not work properly. Therefore the expression in the model controlling the plasma glucose should be replaced with the injected external insulin amount. This can be done with a two-compartment subsystem, where two state variables represent the injected insulin absorption from the subcutaneous layer to plasma [12, 2, 15]. A simplification is to model it with only one compartment, or with a simple absorption function trying to mimic the insulin absorption based on the amount of insulin injected.

A DM2 patient will not always be dependent on external insulin, since the β-cells work, but a person with DM2 who do not control their plasma glucose very well, might also be dependent on external insulin. Therefore the subcutaneous insulin delivery must be included in the model.

UVa/Padova Type 1 Diabetes Simulator The UVa/Padova Type 1 Diabetes Simulator [11, 12] is approved by the U.S Food and Drug Administration as a replacement for animal trials. It is based on a complex metabolic model with many state variables and parameters.

Meal digestion is modelled using a two compartment subsystem to model the stomach, and a third compartment for the gut. This is again transferred from the gut to plasma with a rate of appearance function based on the amount of glucose in the gut and other body parameters. The gastric emptying of glucose from stomach to gut is modelled by a $\tanh$ -function using the amount of glucose in the stomach as input. The digestion subsystem is originally just made for glucose digestion.

The pancreatic insulin secretion is modelled to have a constant basal secretion level during fasting glucose. The insulin secretion is also controlled by the plasma glucose concentration and rate of change of the plasma glucose concentration after meals. The insulin secretion based on the rate of change of the plasma glucose is only working when this rate of change is positive. This is intuitive, as the pancreas can not "take away" or excrete insulin from plasma when the rate of change of plasma glucose is negative. The resulting insulin secreted is seen in the state variable $I_l(t)$, representing insulin in the liver, which is again transferred to plasma with a transfer rate decided by a time constant.

The subcutaneous insulin delivery is modelled with two compartments. The first compartment receives the external insulin, and transfers most of it to a second compartment with a certain rate, and a little straight to plasma. The second compartment transfers the insulin to plasma with another time constant.

The model also has other subsystems like the glucagon subsystem, intraperitoneal insulin delivery, muscle and adipose tissue and more, but these are not relevant for the application described here.

GlucoPred The GlucoPred model is developed by Prediktor Medical. It has 14 state variables and 41 parameters, and is described in more detail in Stige [2].

The digestion is modelled with one compartment for the stomach and one for the gut, with corresponding time constants and body parameters determining the rate of transfer from stomach to gut, and gut to plasma. The meal input to this model is originally just carbohydrate and GI.

The insulin secretion from pancreas is controlled by the plasma glucose concentration and the positive part of the rate of plasma glucose. This is somewhat

similar to the way it's done in the UVa/Padova model. This appears directly in plasma, and not through the liver as in the UVa/Padova model.

The subcutaneous insulin delivery is divided in two pathways, one for "fast" bolus insulin, and one for "slow" basal insulin. Both ways consist of two compartments with time constants, similar to the UVa/Padova approach. In addition to this, it models activity and how this affects the plasma glucose, but this is not relevant here.

Eindhoven Diabetes Education Simulator The Eindhoven Diabetes Education Simulator (E-DES) is based on a simulation model with 6 state variables and 14 model parameters, developed at the Eindhoven University of technology [45]. The model includes equations both for DM1, DM2 and healthy subjects.

The digestion is modelled with one gut compartment. The glucose appearance to this compartment is controlled by a rate of appearance function, which has the meal carbohydrates and time since meal as inputs. From the gut, a model parameter linearly controls the glucose transfer rate to plasma.

The pancreatic insulin secretion is controlled by the plasma glucose concentration, its rate of change and the integral of it. This appears directly in plasma. But it is the remote insulin state variable which controls the glucose use in liver and muscles. The subcutaneous insulin delivery is modelled with a two compartment subsystem, where the second compartment transfers insulin to plasma. The rate of the delivery between the compartments and from the second compartment to plasma is controlled by time constants.

Identifiable Virtual Patient model The Identifiable Virtual Patient model (IVP) [46, 47] is a lower order glycemic model for DM1 patients, consisting of 4 state variables. It is claimed to be identifiable from continuous plasma glucose data.

The meal digestion is modelled by using a rate of appearance function, and a time constant representing the time of the highest point of glucose absorption. This then appears in the ODE for the plasma glucose. This function is a simplification which tries to resemble the rate in which glucose appears in plasma during/after a meal, instead of using an x-compartment model for stomach and gut.

Since this is a model for DM1 patients, pancreatic insulin secretion is not included, and will need to be added to work for a healthy person. External insulin boluses are modelled with one state variable representing the subcutaneous layer, where insulin boluses appears directly. A time constant decides the rate of insulin absorption from the subcutaneous layer to plasma. A state variable, $I_{EFF}(t)$, is used to describe the insulin's effect on the plasma glucose, based on the insulin sensitivity and plasma insulin concentration.

SOGMM The Subcutaneous Oral Glucose Minimal Model (SOGMM), described in Garcia-Tirado et al. [15], is another lower order glycemic model for DM1 patients. It consists of 7 state variables, and is not generally identifiable from continuous plasma glucose measurements.

This model uses one compartment for the stomach and one compartment for the gut, to model the digestion. An absorption constant determines the rate of which the glucose is absorbed from gut to plasma.

Like for the IVP model, since this is used for DM1 patients, insulin secretion in the pancreas is left out, and will need to be added for it to work for healthy subjects. External insulin boluses is modelled very similar to the GlucoPred approach, with two compartments leading up to the plasma insulin. Another state variable represents the amount of insulin in the remote compartment, and affects the plasma glucose concentration, very similar to $I_{EFF}(t)$ in the IVP model.

4.2 Meal parameter estimation

For people with diabetes, it is very important to know what they are eating, and how much of it. It is shown that the accuracy of manual carbohydrate estimation/counting can be low [7, 48, 49, 50]. Therefore, in recent years, dietary aids based on computer vision and image processing have emerged. The goals of these applications are different. Some of them tries to classify the meal or classify different segments of the meal. Others try to estimate the size of the meal, so that the amount of carbohydrates or other nutrients in the meal can be estimated, if the meal type is provided. Some of the most recent applications for meal classifications will be described in section 4.2.1. Meal size estimation will be elaborated on in section 4.2.2. There are also some applications which aim to do both meal classification and carbohydrate estimation at once. These will be described in section 4.2.3.

Some of the applications presented from the articles in this section does more than presented here. In this section it will only be focused on the meal classification and meal size estimation parts. This part will not take into account the problem of checking whether a picture contains food or not. This is because it is a reasonable assumption that a person who wants to find the food amount and nutrients from a picture, actually photographs a meal. Some papers [51, 52] include information about the menu of the restaurant in which the user is taking the meal picture, to help recognize the meal. This and other similar additional information will not be discussed here, as many, if not most, meals are not eaten at a restaurant.

The segmentation of different food on a plate is a prerequisite for some of the algorithms and techniques presented here. Dehais et al. [53] did segmentation by using a deep CNN to create a border map, together with a Seeded Region

Growing method to segment a meal. Segmentation of food will not be the focus in this section.

4.2.1 Meal classification

Schap et al. [8] showed that subjects can identify meals without help pretty well. But many helpful tools based on computer vision and artificial neural networks also exist.

To train meal classifiers one need large datasets with labeled images of food and/or meals. Some of the biggest datasets used for training of these classifiers are ETH Food-101 [54], UEC Food-100 and UEC Food-256 [55]. Many of the applications mentioned here are trained on one or more of these.

Anthimopoulos et al. [56] used an optimized bag-of-features [57] model to classify meals from images. This is a model used in computer vision where image features are gathered, and the frequency of each of the features describes the picture. These features are collected in a visual dictionary used to recognize the features from future meal images. The resulting visual dictionary can be used in a classification algorithm, to determine which food/meal is in the image. Anthimopoulos et al. tried support-vector machine (SVM), artificial neural networks (ANN) and random forests (RF) for this. The overall recognition accuracy of the final version of this application was 77.6%. This was from a dataset of 4868 images collected from the web, where 60% were used for training and 40% for testing.

In the article from Liu et al. [58], a convolutional neural network (CNN) is used to recognize different meals from images. This CNN is implemented on a remote server in the cloud. This makes way for a more complex CNN, which again gives higher classification accuracy and less energy consumption for the mobile device. The bottom layers of the CNN is pre-trained on a dataset called ImageNet [59]. Then the full network is fine-tuned on either of the well known food image datasets. When fine-tuned on the UEC-256, UEC-100 and Food-101 datasets, the top-1 accuracies were 54.5%, 77.5% and 77%, respectively. The top-5 accuracies were 81.8%, 95.2% and 94%.

Kawano et al. [60] presented a smartphone application, FoodCam, capable of recognizing food while the camera points towards it. The user needs to draw bounding boxes around the areas on the screen in which food appears, and the application suggests a list of food so that the user can select the correct one for each bounding box. In the paper it is suggested and tried several different algorithm combinations, with the most accurate having a top-1 accuracy of only 51.9 % on the UEC-100 dataset. Since then, an updated version presented in Yanai et al. [61] got top-1 accuracies of 65.32 % and 52.85 % for UEC-100 and UEC-256, respectively.

The same group [62] also presented an upgrade of FoodCam called Deep-FoodCam, which does the same thing, but implemented with a deep CNN in-

stead of classic computer vision algorithms. This got a top-1 accuracy of approximately 78.77 % and a top-5 accuracy of 95.15 % on UEC-100 dataset.

Hassanejad et al. [63] also implemented a deep CNN to recognize food from meal images. They used a pre-trained Inception v3 network [64], fine tuned on the three datasets UEC-256, UEC-100 and Food-101. During training, distortions were applied to the images in the datasets, so that the training sets became much larger. The top-1 accuracies achieved was 92.56 %, 81.45 % and 88.28 % for the UEC-256, UEC-100 and Food-101 datasets, respectively. The top-5 accuracies was 92.58 %, 97.27 % and 96.88.

Bolaños et al. [65] aimed to do food recognition and classification. Their approach consists of two steps. First, bounding box proposals are generated based on heat map probabilities on the input image. Then, for each bounding box, the present food is classified. The bounding box proposals are generated with a CNN based on GoogleNet, trained on binary food detection. For the food classification, the GoogleNet CNN was re-trained on the Food-101 dataset, before it was fine tuned on the UEC-256 dataset, to be able to classify food from the bounding boxes. The top-1 accuracies achieved was 79.20 % and 63.16 % for the Food-101 and UEC-256 datasets, respectively. The top-5 accuracies were 94.11 % and 85.57 % for the same datasets.

4.2.2 Meal size estimation

Meal size estimation is a very different problem. If one already knows which food is on the plate, a successful meal size estimation can provide the macronutrients in the meal, using a meal composition database.

Stütz et al. [66] used augmented reality on a smartphone application to estimate meal portions of different food. This is done by letting the user manually select the type of food that is to be estimated. Then, by pointing the phone camera towards the meal, the user creates a shape by moving three points. These three points defines a shape which estimates the food shape in 3D. Based on this, the amount of the given food is estimated. A reference marker in the form of a card with the size of a credit card is to be placed next to the plate, for the estimation to work properly. A user study was conducted to measure the performance of the application. The three-point estimation method achieved a relative error of 22.7 % for volume estimation of three different portion sizes of rice. Doomhardt et al. [67] also performed a user study for this application. They reported an improvement in carbohydrate estimation accuracy compared to normal carbohydrate counting for three different meals, for the same group of participants.

Dinic et al. [68] presented an application called EatAR Tango, made for smartphones that have a depth sensor. This way, there are no need to have a special marker next to the plate, because the depth sensor is used to calculate the size of the meal/food. The user takes a photo of the food, and marks the

food on the screen. A 3D grid and a bounding box is created based on the user input. A user study [69] on this application showed reasonably good results, but with a tendency to overestimate (the exact errors were not showed in the article, only in plots). The food estimated were three different portions of rice.

Chae et al. [70] performed volume estimation with shape templates specific for different food. Information about the food gives source to the food template. Together with a segmented food image, features of the food are extracted and a 3D shape reconstructed. The 3D shape is used to determine the volume of the food. On images of beverages (milk an orange juice) and bread slices, the average relative error was 11% for the beverages and 11.7% for the bread slices.

Fang et al. [71] compared two different methods for volume estimation of food. these two were depth image estimation, and estimation from 3D geometric models. These were trained and tested on a image dataset consisting of 10 different food objects. The results showed that using geometric models gave better results than the depth images. Also, the depth images tended to overestimate the volumes. This is in agreement with Dinic et al. [68, 69], where the estimation based on a depth sensor also had a tendency to overestimate the food volumes.

Subhi et al. [72] used a stereo-camera to perform meal size estimation. The stereo camera took two pictures of the meal, from slightly different positions. These were used to estimate the distances from the camera to the different segments of the image. This was used together with the already calculated height and width of the food object to estimate its volume. Four different meals were used for training and testing. Food densities were also found from food databases, to estimate the weight of the food. For the four meals, the average relative estimation errors were 9.1 % and 10.2 %, for volume and weight respectively.

4.2.3 Meal classification and meal size estimation

Another article from Anthimopoulos et al. [73] describes the GoCarb application, which aims to both recognize the meal and estimate the amount. This is also a smartphone application, where the user takes two pictures of the meal. These are used to segment the different food in the meal, recognize them and figure out their 3D shape. From this an estimate of the food amount is made, and the nutritional values can be found from the USDA nutritional database. Only the accuracy of the carbohydrate amount estimation was tested in this study. The mean absolute error of the estimates for 24 different meals, with 12 estimates for each, was 6 ± 8 grams of carbohydrates.

Problems with using these methods in real life, and whether they can be used to get input for a glycemic model, is discussed in section 7.

5 Method

5.1 Data acquisition from Rozendaal

The data from Rozendaal et al. [1] was publicly available in the article's supplementary data. This is data collected from many different studys, where a study group of healthy subjects have eaten a specific meal, in controlled environments. The inclusion criteria for these studies are carefully described in Rozendaal et al. [1]. The data includes the following:

- Grams of aCHO in meal
- PPGR measurements
- Number of subjects
- Glycemic index
- Average age of study group
- Average BMI

In addition to this, for the study meals that it was available, the macronutrient content was collected and used. This means the meals where the macronutrient content were stated in the source article, or the precise meal composition were given, so that macronutrients could be looked up and calculated.

The resulting dataset were a collection of PPGRs (Measurements at 0, 15, 30, 45, 60, 90 and 120 minutes after meal) for different study groups, with the corresponding meal info. The meal info included was available carbohydrates, fat, protein, fiber and glycemic index. The data is included in Appendix A.1.

5.2 Continuous glucose measurements

In addition to the data collected from Rozendaal et al., continuous glucose measurements from two subjects were carried out. These were conducted with a FreeStyle Libre sensor together with a FreeStyle libre reader [74]. The sensors and reader were provided by Prediktor Medical AS. Since each sensor lasts for 14 days, each subjects measured their glucose concentration levels for this period of time. The FreeStyle Libre sensor recorded the plasma glucose concentration every 15 minutes. The measurements were conducted in the subjects' daily lifes.

5.2.1 Test subjects

The glucose measurements were performed on two volunteers, both healthy. Here follows a short description of both subjects.

Subject 1 Male, 25 years old, non-diabetic, frequently exercising, BMI: 20-25.

Subject 2 Female, 23 years old, non-diabetic, frequently exercising, BMI 20-25.

5.2.2 Meal information recording

During the 14 day period of glucose measurements, meal information was recorded. For all of the major meals during the day (breakfast, lunch, dinner and evening meal), the following information was noted:

- Time of meal intake
- Meal composition
- Meal macronutrient content (carbohydrates, fat, protein and fiber)
- Physical activity before/during/after meal (could disturb the data)
- Other relevant info

5.2.3 Choice of meals/input

To get sufficient results, the subjects tried to eat meals which differed with regard to the macronutrient composition. This means that the amount of carbohydrates, fat, proteins and fiber was different from meal to meal. The reason for this was to get a sufficiently rich and variable input. This way the impact of different amounts of macronutrients could be investigated more thoroughly, and it would be easier to estimate the model parameters more precisely.

From the data in the Excel table presented in figures Appendix A.3 and Appendix A.4, one can observe a difference in the subject 1 and subject 2 meal compositions. The average amount of recorded aCHO for each meal for subject 1 was $71.0g$, while it was $19.5g$ for subject 2. At the same time, the amount of recorded fat and protein was $18.0g$ and $26.8g$ for subject 1, and $10.9g$ and $21.5g$ for subject 2. This shows that the relative amount of fat and protein compared to aCHO were much higher for subject 2 than for subject 1. This data also shows that the meal sizes were higher for subject 1 than for subject 2.

5.2.4 Glucose data formatting

The measured glucose data was imported to excel using the FreeStyle Libre Software [75]. The glucose measurements after meal intake were collected and matched up against the meal and meal info, from section 5.2.5. Since the measurements were taken every 15 minutes, the after meal measurement times varied for each meal. The meals and glucose responses that were not interrupted

or disturbed for some reason, were collected and used. The resulting dataset is included in Appendix A.2, in figure Appendix A.3 and Appendix A.4.

5.2.5 Meal info

The meal info written down during the glucose measurement period contained information about what time of day the meal was eaten, and the amount of available carbohydrates, fat, protein and fiber it contained. The smartphone application Lifesum [76] was used to write down and keep control over the meals. To calculate the macronutrient composition of the meals both Lifesum and Matvaretabellen [77] was used as aids.

5.3 PLSR analysis

From the articles that Rozendaal et al. [1] (Rozendaal et al. [1] will from this point on just be referenced to as "Rozendaal") gathered their data, information about each meal was collected, as described in section 5.1. The subject 1 and 2 glucose measurements and meal info were collected in datasets as described in 5.2. For both the data from Rozendaal and the subject measurements, the incremental area under curve (iAUC) were calculated and part of the analysis.

The meal datasets were imported into Unscrambler X [78], for analysis. The built-in PLSR analysis in Unscrambler X was used to find out whether the meal macronutrient amounts and GI could explain the glucose responses to each meal. The NIPALS [79] and the kernel PLS [80] algorithms were used to build the PLSR models. The NIPALS algorithm was applied when the response data Y contained two or more columns and there were occasional missing data, like for the PPGRs from Rozendaal. The kernel PLS was applied for response data Y with one column and no missing data, like the calculated iAUC data from Rozendaal or the subject data.

For the prediction results, a k-fold cross validation scheme with random validation sets and $k = 20$ was used to validate the results. This was the default cross validation method in Unscrambler X. The output of the PLSR was several plots describing different aspects of the regression model and prediction results, like explained in section 2.1.

5.4 Prediction models

From the models presented in section 4.1.2, two models were chosen as suitable to use in the implementation of a glycemic response calculator. Those two models were the IVP model and SOGMM. The main reason that these two were chosen was the low model orders and complexities, compared to the rest of the models. Since the goal with the glycemic response calculator was to try to

predict the plasma glucose response of a subject, high identifiability was important. Low model order and low complexity often means higher chance of estimating the parameters accurately.

Another criteria for the model choosing was the glycemic predictability of the models. The more complex models (UVa/Padova, GlucoPred and E-DES) might get more accurate predictions if the model parameters are estimated correctly. This is because the higher complexity comes from modelled dynamics which hopefully makes the model behave more similar to the real system. Unfortunately, these models are too complex to be identifiable from glucose measurements, without setting a lot of the model parameters constant, which again means assuming things about the real system in our model.

On the other end of the complexity scale, one can look at the Bergman minimal model [10]. This is a model with three state variables and three parameters, as described earlier. It is identifiable, but since it is so simple, it will most likely not be able to predict plasma glucose values very well. Also, some alterations would have been necessary for it to work as a prediction and simulation model. This would have made it look more like the two models already chosen, IVP and SOGGM, which are based on the minimal model itself.

In the following, the IVP and SOGMM models will be altered based on the results from the PLSR analysis. Even though GI showed to be an important meal parameter in that analysis, it will not be a part of the alterations of the models. The reason for this is that GI is not very easy to obtain for all kinds of meals, including the meals in the datasets for subject 1 and 2. The goal of this project is to let people with DM1 or DM2 be able to predict their PPGR based on meal parameters. Then it is better to leave the GI out of the model prediction, even though it would have been interesting to see whether the predictions would have been better.

5.4.1 IVP model alterations and presentation

The original ODEs for the IVP model:

$$\dot{I}_{SC}(t) = -\frac{1}{\tau_1} I_{SC}(t) + \frac{1}{\tau_1} \frac{ID(t)}{C_I} \tag{5.1}$$

$$\dot{I}_p(t) = -\frac{1}{\tau_2} I_p(t) + \frac{1}{\tau_2} I_{SC}(t) \tag{5.2}$$

$$\dot{I}_{EFF}(t) = -p_2 I_{EFF}(t) + p_2 S_I I_p(t) \tag{5.3}$$

$$\dot{G}(t) = -(GEZI + I_{EFF}(t))G(t) + EGP + R_A(t) \tag{5.4}$$

$$R_A(t) = \frac{C_H(t)}{V_G \tau_m^2} t e^{-\frac{t}{\tau_m}} \tag{5.5}$$

Where the state variables are the subcutaenous insulin concentration (I_{SC}),

insulin in plasma (I_p), insulin effect (I_{EFF}) and plasma glucose (G). The model parameter values are given in table Appendix A.1. This model was originally made to model diabetes 1 patients. Therefore there is no pancreatic insulin secretion controlling the plasma glucose. To model this for a healthy person, two expressions are added to the ODE for I_p, plasma insulin. This leads to the following ODE for I_p for healthy subjects:

$$\dot{I_p}(t) = -\frac{1}{\tau_2} I_p(t) + \frac{1}{\tau_2} I_{SC}(t) + k_1 \dot{G(t)}^+ + k_2 G(t) \tag{5.6}$$

Where k_1 and k_2 are parameters determining the rate of glucose dependent insulin secretion in the pancreatic β-cells. $\dot{G(t)}^+$ means that only the positive part of $\dot{G(t)}$ counts, and the negative part is zero.

Based on the PLSR analysis results presented in section 6.1, a possible model alteration to take into account the amount of fat, protein and fiber (from here on called "FPF") in a meal is to use the sum of the three, from here on called S_{FPF}.

$$S_{FPF} = a_{fat} + a_{protein} + a_{fiber} \tag{5.7}$$

Where a_{fat}, $a_{protein}$ and a_{fiber} means the amount of fat, protein and fiber in grams. The time constant, τ_m, determining the height and length of the curve $R_A(t)$ creates, can be determined by S_{FPF}. A suggestion for the new $R_A(t)$ is:

$$R_A(t) = \frac{C_H(t)}{V_G \tau_m^2} t e^{-\frac{t}{p_\tau \tau_m}} \tag{5.8}$$

where τ_m can be related to the amount of FPF in different ways.

$$\tau_m = p_m(1 + S_{FPF}) \tag{5.9}$$
$$\tau_m = p_m(1 + S_{FPF})^2 \tag{5.10}$$
$$\tau_m = p_m\sqrt{1 + S_{FPF}} \tag{5.11}$$

This way the new parameters p_τ and p_m can be estimated to determine the shape and size of $R_A(t)$. The area under the curve for $R_A(t)$ varies with the value of p_τ, and p_m is a value representing how much the FPF affects the PPGR. The reason that 1 is added to S_{FPF} in equations (5.9)-(5.11) is so that τ_m will never be zero, even though $S_{FPF} = 0$, like it would be for an OGTT. Other ways it could be modelled is:

$$\tau_m = p_{m1} + p_{m2} S_{FPF} \tag{5.12}$$
$$\tau_m = p_{m1} + p_{m2} S_{FPF}^2 \tag{5.13}$$
$$\tau_m = p_{m1} + p_{m2} \sqrt{S_{FPF}} \tag{5.14}$$

This would increase the possibilities for the values of τ_m based on the FPF, and therefore a better chance of mimic glucose curves from real measurements. But, this would also introduce one more model parameter in the model. Therefore equations (5.9)-(5.11) were chosen as the ones to be used during the parameter estimation.

The resulting model equations are the following:

$$\dot{I}_{SC}(t) = -\frac{1}{\tau_1} I_{SC}(t) + \frac{1}{\tau_1} \frac{ID(t)}{C_I} \tag{5.15}$$
$$\dot{I}_p(t) = -\frac{1}{\tau_2} I_p(t) + \frac{1}{\tau_2} I_{SC}(t) + k_1 \dot{G(t)}^+ + k_2 G(t) \tag{5.16}$$
$$\dot{I}_{EFF}(t) = -p_2 I_{EFF}(t) + p_2 S_I I_p(t) \tag{5.17}$$
$$\dot{G}(t) = -(GEZI + I_{EFF}(t))G(t) + EGP + R_A(t) \tag{5.18}$$
$$R_A(t) = \frac{C_H(t)}{V_G \tau_m^2} t e^{-\frac{t}{\tau_m}} \tag{5.19}$$

5.4.2 SOGMM model alterations and presentation

The original ODEs for the SOGMM model:

$$\dot{x}_1(t) = -(S_g + x_2(t))x_1(t) + S_g G_b + \frac{k_{abs} f}{BW \cdot V_g} x_4(t) \tag{5.20}$$
$$\dot{x}_2(t) = -p_2 x_2(t) + p_2 S_I (I(t) - I_b) \tag{5.21}$$
$$\dot{x}_3(t) = -k_\tau x_3(t) + \omega(t) \tag{5.22}$$
$$\dot{x}_4(t) = -k_{abs} x_4(t) + k_\tau x_3(t) \tag{5.23}$$
$$\dot{x}_5(t) = -k_d x_5(t) + J_{ctrl}(t) \tag{5.24}$$
$$\dot{x}_6(t) = -k_d x_6(t) + k_d x_5(t) \tag{5.25}$$
$$\dot{x}_7(t) = -k_{cl} x_7(t) + k_d x_6(t) \tag{5.26}$$

Where the state variables are plasma glucose concentration (x_1), proportion of insulin in remote compartment (x_2), glucose mass in stomach (x_3), glucose mass in gut (x_4), injected insulin in the first compartment (x_5), second compartment (x_6) and plasma insulin (x_7). The model parameter values are given

in table Appendix A.2. Also this model was originally for DM1 patients. The pancreatic insulin secretion can be added like for the IVP model:

$$\dot{x}_7(t) = -k_{cl}x_7(t) + k_d x_6(t) + k_1 \dot{G(t)}^+ + k_2 G(t) \tag{5.27}$$

Suggested alterations to take fat, protein and fiber into account is to let both k_τ and k_{abs} be affected by S_{FPF}. These are inverse time constants determining the glucose transfer rate from stomach to gut, and from gut to plasma, respectively. Therefore, again based on analysis results from section 6.1, they should be inversely correlated to S_{FPF}:

$$k_\tau = \frac{p_{k\tau}}{1 + S_{FPF}} \tag{5.28}$$

$$k_{abs} = \frac{p_{kabs}}{1 + S_{FPF}} \tag{5.29}$$

The digestion rate can be related to FPF in different ways also here:

$$k_\tau = \frac{p_{k\tau}}{(1 + S_{FPF})^2} \tag{5.30}$$

$$k_\tau = \frac{p_{k\tau}}{\sqrt{1 + S_{FPF}}} \tag{5.31}$$

Also for the SOGMM model, other ways of modelling the digestion rate were considered, like in equations (5.12)-(5.14) for IVP. But the introduction of additional model parameters made the equations (5.28), (5.30) and (5.31) a better choice.

The resulting model equations are the following:

$$\dot{x}_1(t) = -(S_g + x_2(t))x_1(t) + S_g G_b + \frac{k_{abs} f}{BW \cdot V_g} x_4(t) \tag{5.32}$$

$$\dot{x}_2(t) = -p_2 x_2(t) + p_2 S_I (I(t) - I_b) \tag{5.33}$$

$$\dot{x}_3(t) = -k_\tau x_3(t) + \omega(t) \tag{5.34}$$

$$\dot{x}_4(t) = -k_{abs} x_4(t) + k_\tau x_3(t) \tag{5.35}$$

$$\dot{x}_5(t) = -k_d x_5(t) + J_{ctrl}(t) \tag{5.36}$$

$$\dot{x}_6(t) = -k_d x_6(t) + k_d x_5(t) \tag{5.37}$$

$$\dot{x}_7(t) = -k_{cl}x_7(t) + k_d x_6(t) + k_1 \dot{G(t)}^+ + k_2 G(t) \tag{5.38}$$

5.4.3 Model parameter sensitivity analysis

The model identifiability was investigated using sensitivity analysis. The two chosen glycemic models were implemented in Matlab, using a simulation time

step of 0.5 minutes. The model equations included the alterations added in sections 5.4.1 and 5.4.2.

The sensitivity analysis was carried out running equations (2.3) and (2.4) parallel with the model simulation. When the sensitivity matrix $\mathbf{S}$, described in section 2.4, was built, a singular value decomposition was performed on it. From this, the right singular vectors (RSV) corresponding to the highest singular values could be plotted to observe which model parameters had the highest sensitivity.

A parameter ranking, called V_{sum} here, (Also described in Stige [2]) was used as a tool to help decide the most sensitive parameters. The sum of RSV-contribution weighted by the corresponding singular values for each parameter was computed and plotted. This made sure the highest singular values contributed most when selecting identifiable parameters based on it, and that lower singular values did not.

To make sure the input (aCHO, fat, protein and fiber) to the sensitivity analysis were realistic, the data from Rozendaal, subject 1 and subject 2 were used as inputs.

For the IVP model, the parameters t_1 and C_I was not considered in the sensitivity analysis, as no subcutaneous insulin was part of the input for the healthy data. For the same reson, the parameter k_d was not considered for the SOGMM model. The distribution volume of glucose, V_g, was taken out in both models, because it can be estimated accurately from the height and weight of the subject. Also the body weight BW was taken out because it can be measured to reasonable precision. For both models, only the model with linear FPF relation to carbohydrate digestion rate ((5.9) and (5.28)) was used in the sensitivity analysis.

5.4.4 Parameter estimation and prediction

The model parameter estimation was carried out for the two models and the parameter sets selected from the sensitivity analysis (Equations (6.1) and (6.2)). The parameter estimation technique implemented was the Downhill Simplex (Nelder-Mead) algorithm. The boxcar function was used instead of the $d_{x,i}$ described in equation (2.8). This was because during the initial estimation testing, the $d_{x,i}$ produced a parameter value bias, while the boxcar function did not. The $d_{x,i}$ from (2.8) dragged the parameter estimations towards the middle of the parameter ranges, despite the better parameter value being somewhere else in the parameter range.

The training was done by estimating the model parameters in (6.1) or (6.2) for one subject input and the corresponding PPGRs. The parameter values, $P_{cal,i}$, for one calibration set, S_i, was found by calculating the average of the parameter values, weighted by the desirability for each estimation:

$$P_{cal,i} = \frac{\sum_{j=1}^{n_{cal}} d_j P_{est,j}}{\sum_{j=1}^{n_{cal}} d_j} \tag{5.39}$$

Where d_j is the desirability for the parameter estimation $P_{est,j}$ on meal j in the calibration set. n_{cal} is the number of meals in the calibration set. This way, the bad estimations did not count as much to the final parameter values as the better estimations did.

To validate the predictions, a leave-one-out cross validation scheme was used. For each training round, one meal was picked for the prediction validation set, and the rest was used to train/calibrate the model. Each meal was picked in the validation set once. The validation was measured using the desirability value for a simulation with the new parameters $P_{cal,i}$ against the reference PPGR of the validation meal that was held out of the calibration set.

6 Results and observations

6.1 PLSR analysis

The results from the PLSR analysis, both from Rozendaal data and the subject measurements, are presented in the following. Table 6.1 presents the calibration and validation results in the form of the EV from the PLSR analysis, as well as the important and not important input variables in the model. Figure 6.1 shows the plots of the EVs for the factors of the PLSR models, and for the different combinations of input and response.

One can observe that when the response variable Y = PPGR (Plots 6.1a and 6.1b, and row 1-7 in table 6.1), the EV is in the same range of values for all inputs, except the input not containing the GI. For the inputs including the GI, the explained variance is between $40 - 50\%$ for both the calibration and validation sets. The one input without GI has an EV of 34.1% for the validation set. Another interesting result is that replacing the three variables fat, protein and fiber with the sum of them, S_{FPF}, did not decrease the EV significantly for the Rozendaal data. Using S^2_{FPF} or $\sqrt{S_{FPF}}$ gave approximately the same results.

One can see that the GI is always a part of the important input variables, when it is a part of the input. An example of this is shown in the plot in figure 6.2, where GI is the input variable closest to the outer circle. From the figures 6.2 and 6.3 one can see from how close they are placed in the plots, that there is correlation between aCHO, GI and PPGR, and between aCHO and iAUC. The same way one can see that fat, protein and fiber anticorrelates with PPGR and iAUC over factor-1. This can indicate that when fat, protein and fiber is higher, the PPGR is lower or slower, and vice versa.

Another thing to observe is that fiber is almost always a part of the less important input to the model, when it is an input. The only exception is for subject 2, where it actually turned out to be the most important variable, as can be seen in figure 6.5. For the rest of the input, this indicates that fiber is not so significant when trying to predict the PPGR after a meal.

When the response variable Y = iAUC (Plots 6.1c and 6.1d, and row 8-17 in table 6.1), the results were very similar with or without GI for the Rozendaal data, but only with 33.6% and 33.5% in calibration EV. For subjects 1 and 2, using the macronutrient composition gave higher calibration EV than for the Rozendaal data, but the validation EVs were much lower. When using the sum of fat, protein and fiber (S_{FPF}) as input, instead of each one on their own, the validation EV was slighty worse for subject 1, but more than halved for subject 2. Using S^2_{FPF} gave slightly worse results than for S_{FPF} for both subjects, while using $\sqrt{S_{FPF}}$ gave slightly better.

In figure 6.4 one can observe that for subject 1, fat, protein and fiber anticorrelates with iAUC over factor-2. Figure 6.5 shows that for subject 2, aCHO

and iAUC correlates, but so does fiber and iAUC. Fat and protein slightly anti-correlates with iAUC over factor-2. This is a much different correlation loadings plot than most of the others, since fiber correlates more with iAUC and aCHO is not looking like an important input variable.

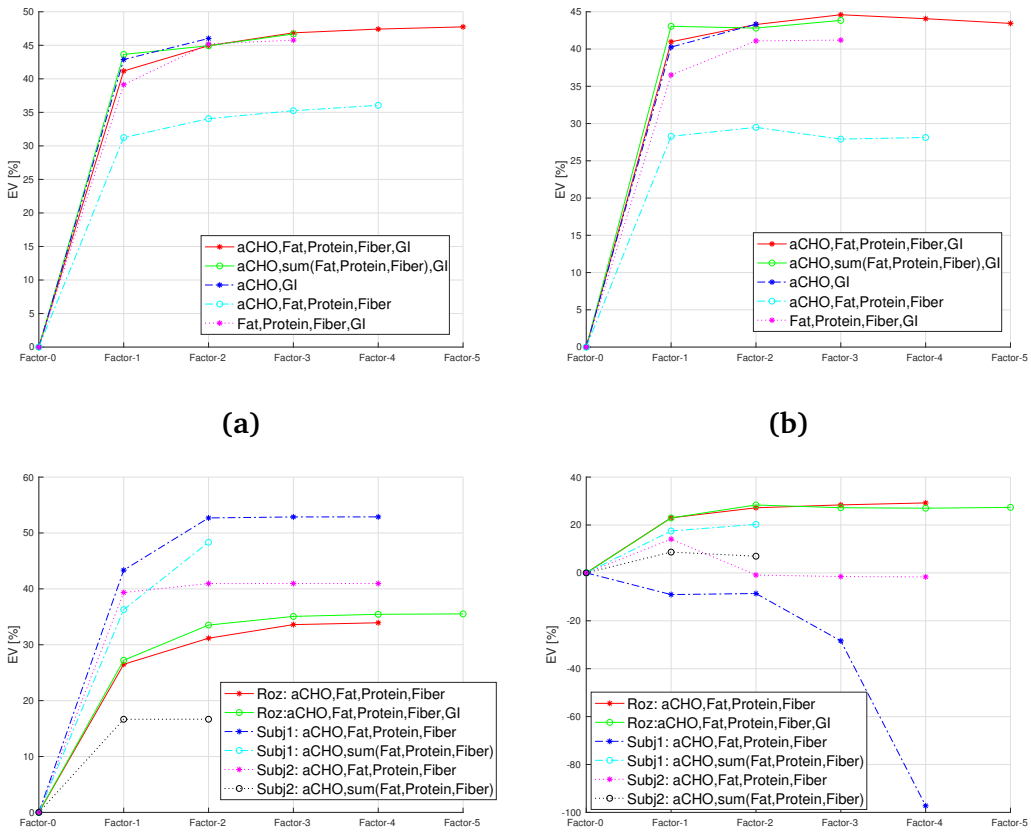

Figure 6.1: Explained variance for the different PLSR-inputs X.
(a) For calibration set, with X described in legends and Y = PPGRs. Data only from Rozendaal.
(b) For validation set, with X described in legends and Y = PPGRs. Data only from Rozendaal.
(c) For calibration set, with X described in legends and Y = iAUC.
(d) For validation set, with X described in legends and Y = iAUC.

Input X	**Response** Y	**Cal EV***	**Val EV****	**Important** X	**Not important** X
Roz: aCHO, fat, protein, fiber, GI	PPGR	46.8%	44.6%	Fat, protein, GI	Fiber
Roz: aCHO, S_{FPF} ***, GI	PPGR	46.7%	43.8%	aCHO, S_{FPF}, GI	
Roz: aCHO, S^2_{FPF}, GI	PPGR	46.7%	42.0%	aCHO, GI	
Roz: aCHO, $\sqrt{S_{FPF}}$, GI	PPGR	46.4%	43.4%	aCHO, $\sqrt{S_{FPF}}$, GI	
Roz: aCHO, GI	PPGR	46.0%	43.3%	aCHO, GI	
Roz: aCHO, fat, protein, fiber	PPGR	34.1%	29.5%	aCHO, fat, protein	Fiber
Roz: Fat, protein, fiber, GI	PPGR	45.8%	41.2%	Fat, protein, GI	Fiber
Roz: aCHO, fat, protein, fiber	iAUC	33.6%	28.4%	aCHO, fat, protein	Fiber
Roz: aCHO, fat, protein, fiber, GI	iAUC	33.5%	28.4%	aCHO, fat, protein, GI	Fiber
Subj1: aCHO, fat, protein, fiber	iAUC	52.7%	-8.6%	aCHO, protein	Fiber
Subj1: aCHO, S_{FPF}	iAUC	48.3%	20.3%	aCHO, S_{FPF}	
Subj1: aCHO, S^2_{FPF}	iAUC	39.6%	14.7%	aCHO, S^2_{FPF}	
Subj1: aCHO, $\sqrt{S_{FPF}}$	iAUC	48.6%	22.2%	aCHO, $\sqrt{S_{FPF}}$	
Subj2: aCHO, fat, protein, fiber	iAUC	39.4%	14.1%	Fiber	aCHO, protein
Subj2: aCHO, S_{FPF}	iAUC	16.7%	8.7%	aCHO, S_{FPF}	
Subj2: aCHO, S^2_{FPF}	iAUC	16.7%	-0.9%	aCHO, S^2_{FPF}	
Subj2: aCHO, $\sqrt{S_{FPF}}$	iAUC	17.3%	9.4%	aCHO, $\sqrt{S_{FPF}}$	

Table 6.1: PLSR results.
The two last columns describes the important and not important input variables X in the prediction of response variables Y, based on the correlation loadings plots.
* The calibration set's explained variance for the factor corresponding to the highest explained variance in the validation set.
** The highest explained variance in the validation set.
*** Means the sum of fat, protein and fiber in the meal.

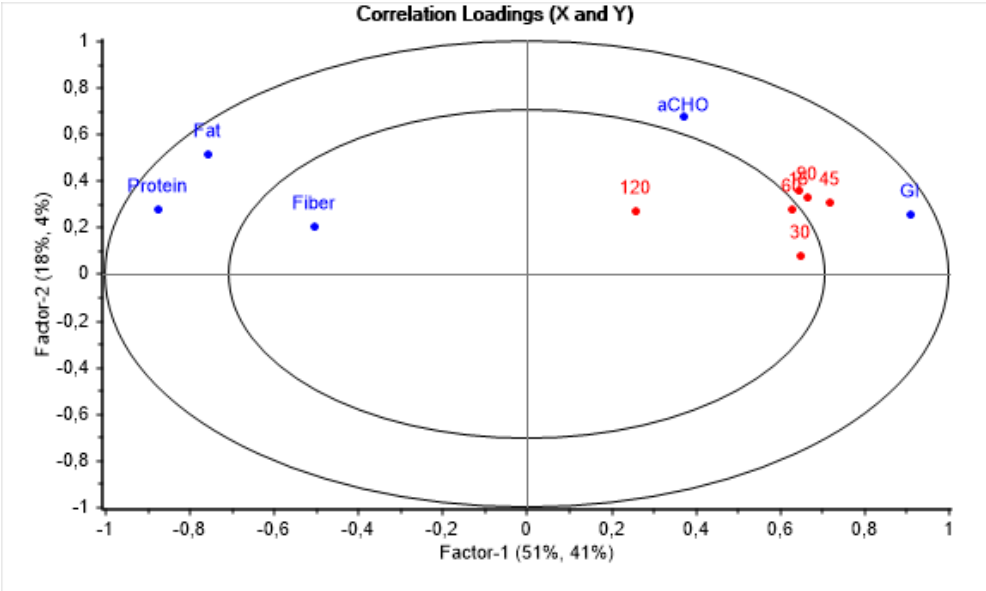

Figure 6.2: Corr. loadings plot Rozendaal. X = aCHO, fat, protein, fiber and GI. Y = GR.

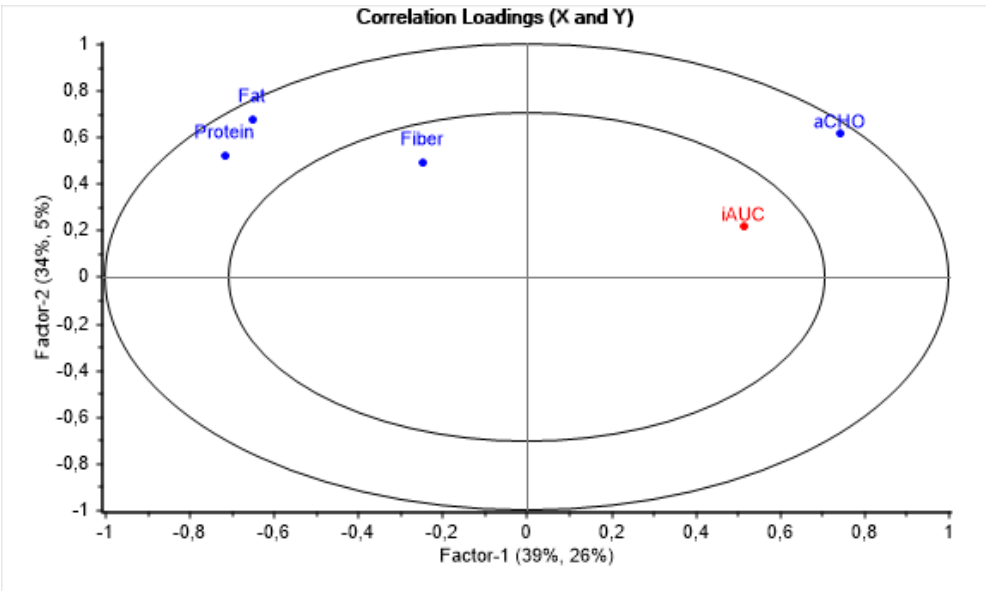

Figure 6.3: Corr. loadings plot Rozendaal. X = aCHO, fat, protein and fiber. Y = iAUC.

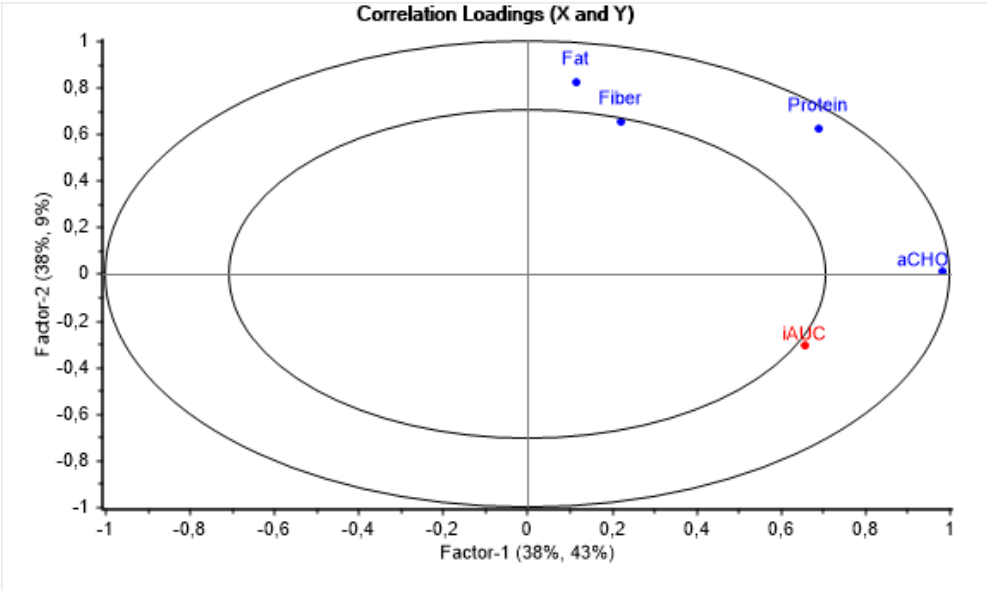

Figure 6.4: Corr. loadings plot subject 1. X = aCHO, fat, protein and fiber. Y = iAUC.

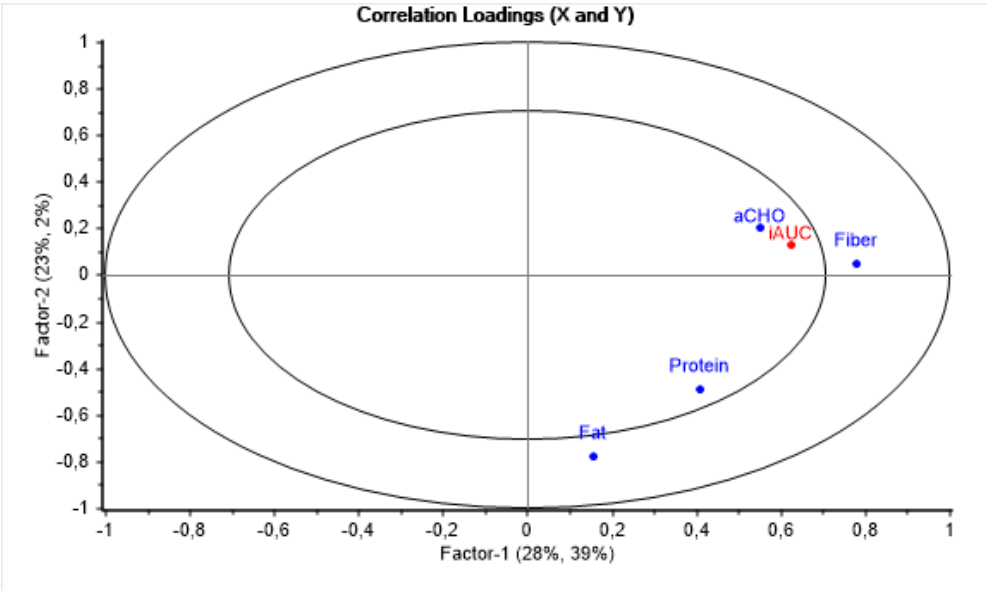

Figure 6.5: Corr. loadings plot subject 2. X = aCHO, fat, protein and fiber. Y = iAUC.

6.2 Model parameter sensitivity analysis

In this section the results from the model parameter sensitivity analysis is presented. This was done for both the IVP and SOGMM models, as described in section 5.4.3.

6.2.1 IVP sensitivity analysis

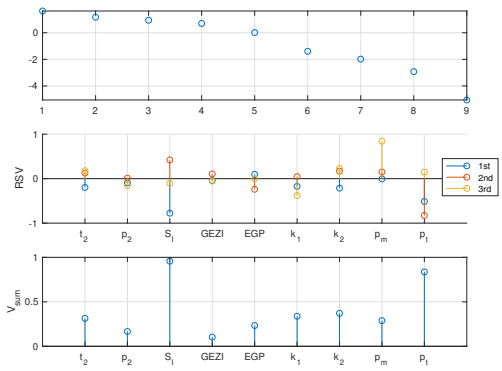

(a)

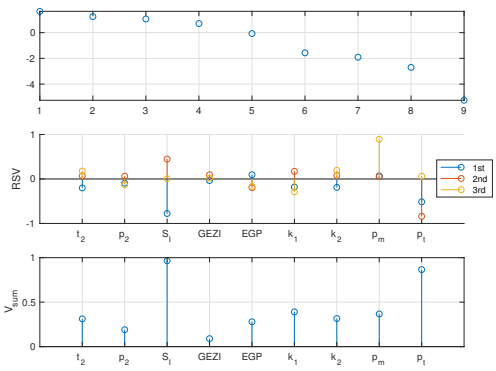

(b)

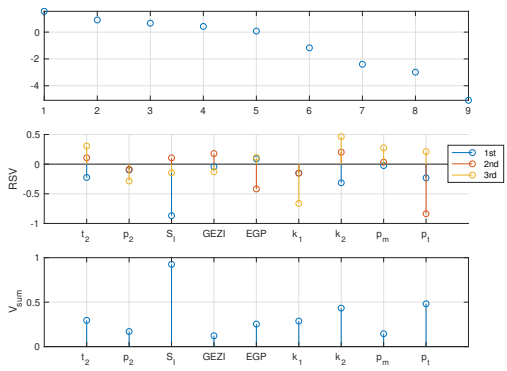

(c)

Figure 6.6: IVP model parameter sensitivity plots. Upper plots: Singular values of the sensitivity matrix **S**. Middle plots: The RSVs corresponding to the three highest singular values. Lower plots: V_{sum} values.
(a) Model parameter sensitivity plot with all input, for IVP model with all parameters.
(b) Model parameter sensitivity plot with subject 1 input, for IVP model with all parameters.
(c) Model parameter sensitivity plot with subject 2 input, for IVP model with all parameters.

The IVP model parameter sensitivity analysis was carried out with all relevant parameters. The sensitivity plot is showed in figure 6.6a. The parameters p_2, $GEZI$, EGP and p_m had the lowest V_{sum} values. Since p_m is a new parameter, added to explain responses to fat, protein and fiber, this stayed in the parameter set, while the three others were removed. The following parameter set was left to identify in the parameter estimation part.

$$P_{IVP} = [t_2, S_I, k_1, k_2, p_m, p_t] \tag{6.1}$$

An interesting observation from the sensitivity analysis is the difference in parameter sensitivity for different input. The figures 6.6b and 6.6c shows the sensitivity plots for subject 1 and subject 2 input, respectively. For the subject 1 input, where the amount of aCHO were high compared to the other macronutrients, the parameters p_m and p_t showed higher sensitivity than for the subject 2 input, where aCHO amount were lower compared to the other macronutrients.

6.2.2 SOGMM sensitivity analysis

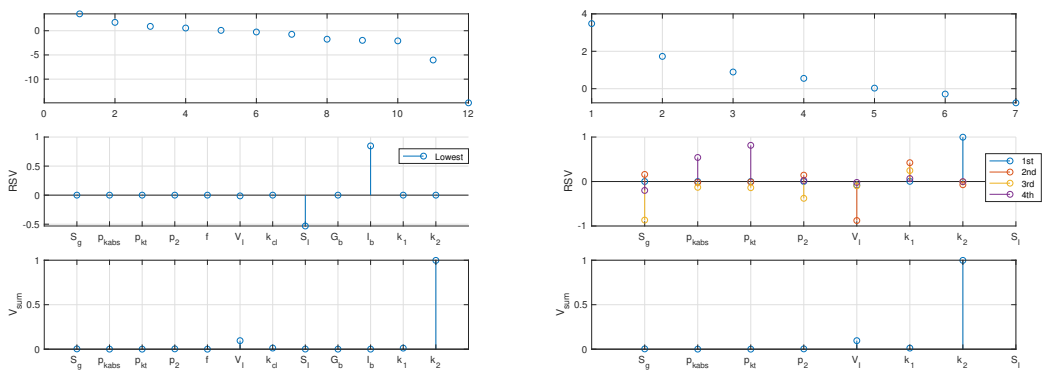

(a) **(b)**

Figure 6.7: SOGMM model parameter sensitivity plots, for all input. Upper plots: Singular values of the sensitivity matrix **S**. Middle plots: RSVs. Lower plots: V_{sum} values.
(a) Model parameter sensitivity plot for SOGMM model with all parameters. RSV for the lowest singular value.
(b) Model parameter sensitivity plot for SOGMM model with selected parameters. RSVs for the three highest singular values.

The SOGMM model parameter sensitivity analysis was carried out with all the relevant parameters.

Because the amount of parameters were higher for this model, the least sensitive parameters were removed one by one based on the sensitivity plots. In

figure 6.7a, two parameters, S_I and I_b, contributes to the RSV corresponding to the lowest singular value. Since I_b contributed the most, this was removed, and therefore set constant for the parameter estimation. This approach was used until a suitable number of parameters were left, based on the plot of singular values from the sensitivity matrix. The removed parameters based on this procedure were I_b, f, S_I, G_b and k_{cl}. The parameter set to estimate in the parameter estimation part then ended up as:

$$P_{SOGMM} = [S_g, p_{kabs}, p_{kt}, p_2, V_I, k_1, k_2] \tag{6.2}$$

6.3 Model parameter estimation

	Linear		**Quadratic**		**Square root**		**None**	
Par	**Subj 1**	**Subj 2**	**Subj 1**	**Subj 2**	**Subj 1**	**Subj 2**	**Subj 1**	**Subj 2**
t_2	29.9	42.9	40.8	55.0	49.5	43.9	36.9	44.1
S_I	0.0078	0.0050	0.0060	0.0038	0.0066	0.0047	0.0073	0.0037
EGP							0.67	1.24
k_1	0.45	0.29	0.48	0.36	0.48	0.34	0.67	0.46
k_2	0.0023	0.0019	0.0017	0.0012	0.0021	0.0019	0.0015	0.0015
p_m	1.46	1.07	0.61	0.24	13.9	8.0		
p_t	0.66	0.86	0.77	0.99	1.08	1.03		
t_m							73.6	48.1

Table 6.2: IVP average parameter estimation values. The upmost row means linear, quadratic, square root or no FPF relationship in the model.

The results of the model parameter estimation will be presented here, for both the IVP and SOGMM model. In tables 6.2 and 6.3, the estimated parameter values are presented, based on which input the parameters are estimated for (subject 1 or 2), and the modelled FPF relation to carbohydrate digestion rate (linear, quadratic, square root or none). It can be observed that there is a somewhat consistent pattern for the parameter estimations between subject 1 and 2 input. If a parameter is higher for subject 1 than for subject 2 for one of the FPF relations, it often tends to be that for the others as well.

One can also observe that for the IVP model, the parameter p_m was very different for the different FPF relationships. This is because p_m is the parameter that is multiplied with $\sqrt{S_{FPF}}$, S_{FPF} or S_{FPF}^2 in the model equations. These values will be different from each other, unless $S_{FPF} = 0$. This means that, if the parameter estimation is successful, p_m will be estimated to a different value based on how the FPF relationship is modelled. The same applies to the parameter p_{kt} in the SOGMM model.

	Linear		Quadratic		Square root		None	
Par	**Subj 1**	**Subj 2**	**Subj 1**	**Subj 2**	**Subj 1**	**Subj 2**	**Subj 1**	**Subj 2**
S_g	0.072	0.073	0.097	0.093	0.126	0.098	0.093	0.061
p_{kabs}	2.1	2.5	2.1	2.3	2.3	2.0		
p_{kt}	0.95	3.1	80.5	237.4	0.25	2.59		
k_{abs}							0.037	0.044
k_t							0.019	0.076
p_2	0.048	0.058	0.055	0.060	0.063	0.060	0.046	0.046
V_I	3.7	3.9	3.4	4.1	3.9	4.3	3.4	4.0
k_1	5.3	4.3	5.0	4.9	3.7	4.4	5.5	6.2
k_2	2.5	0.7	2.5	0.8	3.2	0.8	2.7	1.0

Table 6.3: SOGMM average parameter estimation values. The upmost row means linear, quadratic, square root or no FPF relationship in the model.

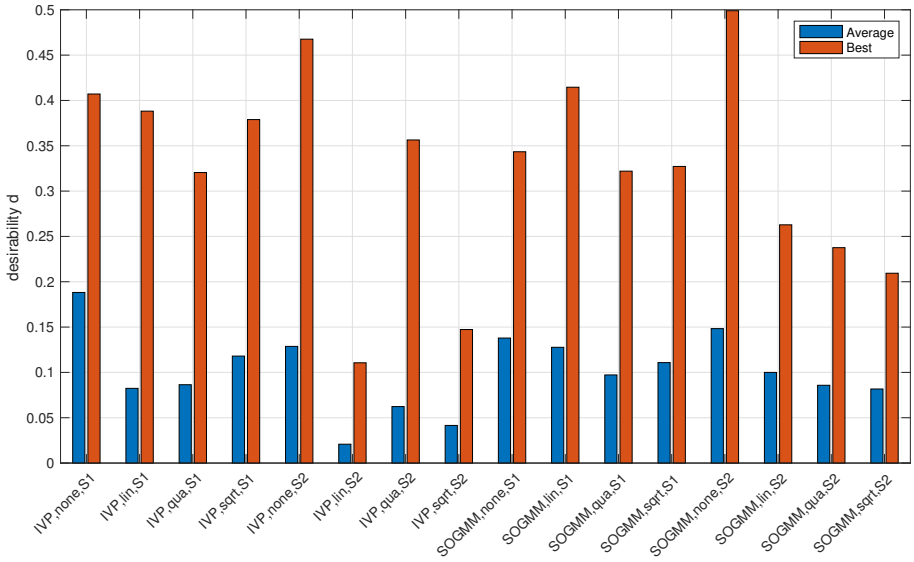

Figure 6.8: Desirability values from predictions for combinations of model (IVP or SOGMM), FPF relationship (None, linear, quadratic or square root) and subject (1 or 2).

Figure 6.8 and table 6.4 shows the desirability results d of the predictions, for every combination of model and input. One can observe that overall, the desirability for the SOGMM predictions are higher than for the IVP predictions. Also, the predictions for subject 1 were generally better than the predictions for subject 2. The best desirability results overall were obtained when the models did not include any sensitivity for fat, protein and fiber.

For subject 1, the best prediction results came from the model without FPF

Model	FPF relationship*	Input	Average d	Best d	Worst d
IVP	-	Subject 1	0.1882	0.4071	0.0040
IVP	Linear	Subject 1	0.0824	0.3882	0.0003
IVP	Quadratic	Subject 1	0.0864	0.3205	0.0000
IVP	Square root	Subject 1	0.1180	0.3789	0.0008
IVP	-	Subject 2	0.1287	0.4676	0.0001
IVP	Linear	Subject 2	0.0208	0.1106	0.0000
IVP	Quadratic	Subject 2	0.0623	0.3564	0.0000
IVP	Square root	Subject 2	0.0415	0.1473	0.0000
SOGMM	-	Subject 1	0.1379	0.3434	0.0027
SOGMM	Linear	Subject 1	0.1277	0.4146	0.0010
SOGMM	Quadratic	Subject 1	0.0972	0.3220	0.0001
SOGMM	Square root	Subject 1	0.1108	0.3272	0.0014
SOGMM	-	Subject 2	0.1483	0.4990	0.0012
SOGMM	Linear	Subject 2	0.1000	0.2628	0.0024
SOGMM	Quadratic	Subject 2	0.0858	0.2376	0.0015
SOGMM	Square root	Subject 2	0.0817	0.2094	0.0019

Table 6.4: Prediction results after parameter estimation.
* Relationship between modelled rate of glucose absorption and fat, protein and fiber content.

relationship modelled. From the rest of the models, the ones that included FPF input, the best prediction gave highest desirability when the relationship between FPF and carbohydrate digestion rate were modelled linearly, for both models. The average desirability values were clearly highest with the square root FPF relationship for the IVP model, and only slightly highest for the linear FPF relationship for the SOGMM model.

For subject 2, the best prediction results also came from the model with no FPF relationship modelled. For the rest, the IVP predictions were clearly best when the FPF relationship were quadratic. For the SOGMM model, the desirability values were pretty similar for all FPF relationships, but the linear one were slightly best.

Figures 6.9 and 6.10 shows the best and worst prediction results for the parameter estimations for the IVP model parameters. Plots 6.9a, 6.9c, 6.10a and 6.10c shows the results for subject 1, and 6.9b, 6.9d, 6.10b and 6.10d for subject 2. For both subject input, the best predictions are pretty similar to the corresponding reference curve, while the worst are not very precise at all. The worst predictions are typically for the reference PPGRs with very high curves, while the best ones are for the much lower reference curves. The exception is for meal 17 on plot 6.9b, where the reference PPGR was relatively high, yet the prediction was fairly accurate.

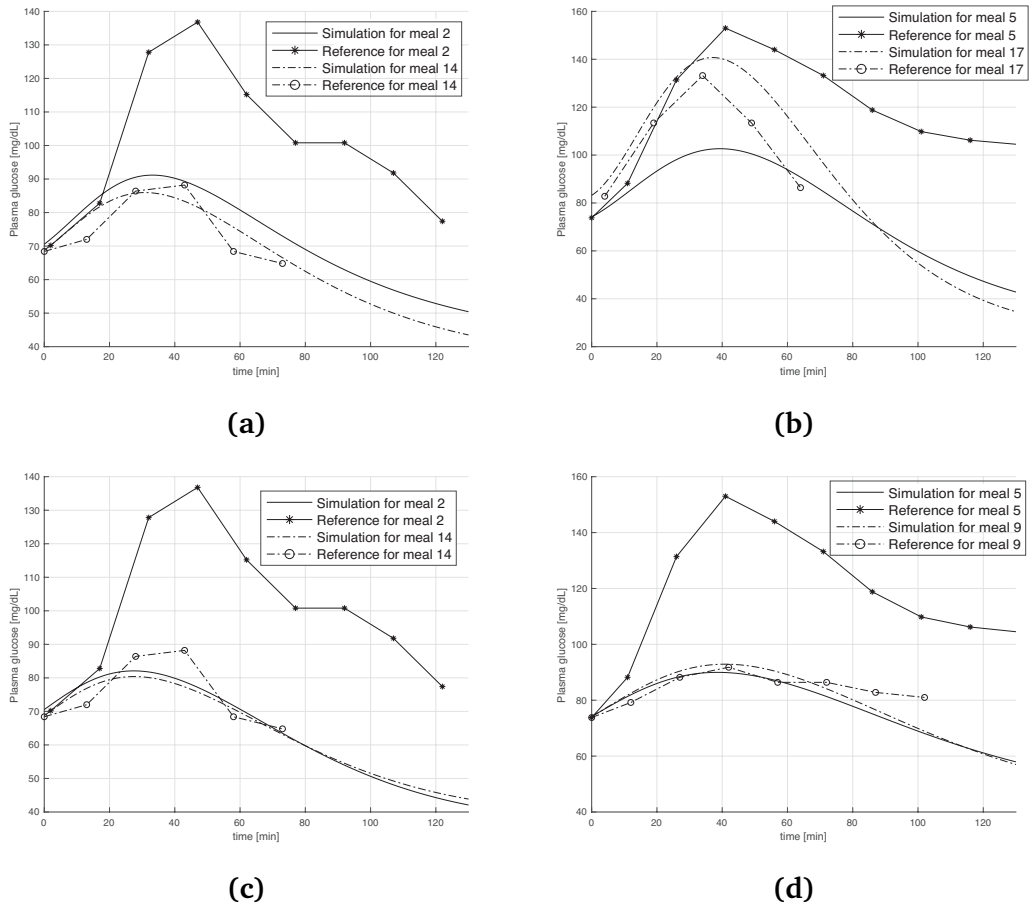

Figure 6.9: IVP model parameter estimation result for best and worst meal, for linear and quadratic FPF relationships.
(a) Reference from subject 1 for meals 2 ($d = 0.0003$) and 14 ($d = 0.3882$), and simulated prediction after parameter estimation, with linear FPF relationship.
(b) Reference from subject 2 for meals 5 ($d = 0.0000$) and 17 ($d = 0.1106$), and simulated prediction after parameter estimation, with linear FPF relationship.
(c) Reference from subject 1 for meals 2 ($d = 0.0000$) and 14 ($d = 0.3205$), and simulated prediction after parameter estimation, with quadratic FPF relationship.
(d) Reference from subject 2 for meals 5 ($d = 0.0000$) and 9 ($d = 0.3564$), and simulated prediction after parameter estimation, with quadratic FPF relationship.

The best and worst prediction results for the SOGMM parameter estimation are shown in figures 6.11 and 6.12. Plots 6.11a, 6.11c, 6.12a and 6.12c shows the results for subject 1, and 6.11b, 6.11d, 6.12b and 6.12d for subject 2. The

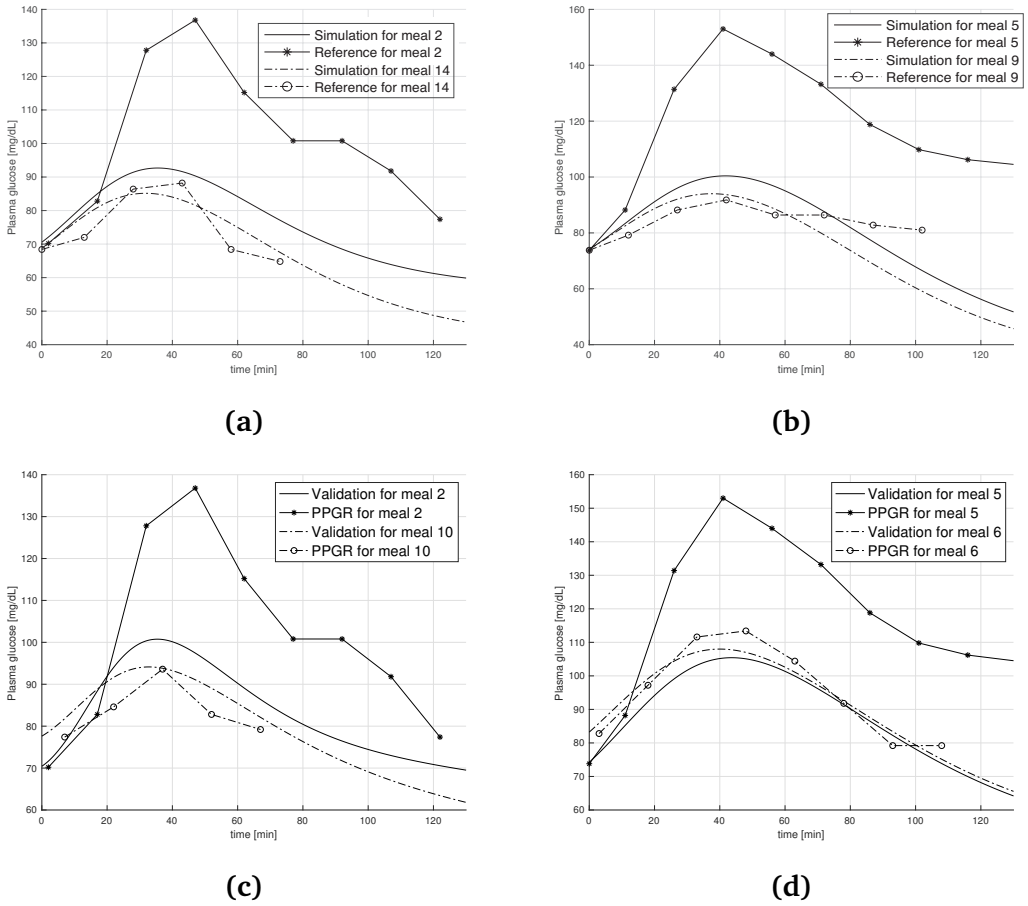

Figure 6.10: IVP model parameter estimation result for best and worst meal.
(a) Reference from subject 1 for meals 2 ($d = 0.0008$) and 14 ($d = 0.3789$), and simulated prediction after parameter estimation, with square root FPF relationship.
(b) Reference from subject 2 for meals 5 ($d = 0.0000$) and 9 ($d = 0.1473$), and simulated prediction after parameter estimation, with square root FPF relationship.
(c) Reference from subject 1 for meals 2 ($d = 0.0040$) and 10 ($d = 0.4071$), and simulated prediction after parameter estimation, with no FPF relationship.
(d) Reference from subject 2 for meals 5 ($d = 0.0001$) and 6 ($d = 0.4676$), and simulated prediction after parameter estimation, with no FPF relationship.

best and worst predictions are shown in each plot, like for the IVP model. Also here, the best predictions are pretty good, while the worst are not very accurate. The results showed for meal 7 in the subject 1 plots are different from the other worst results. Here the error lies mostly in that the predicted response comes

too early too fit the reference. The other worst predictions often just predicted a response that was too low.

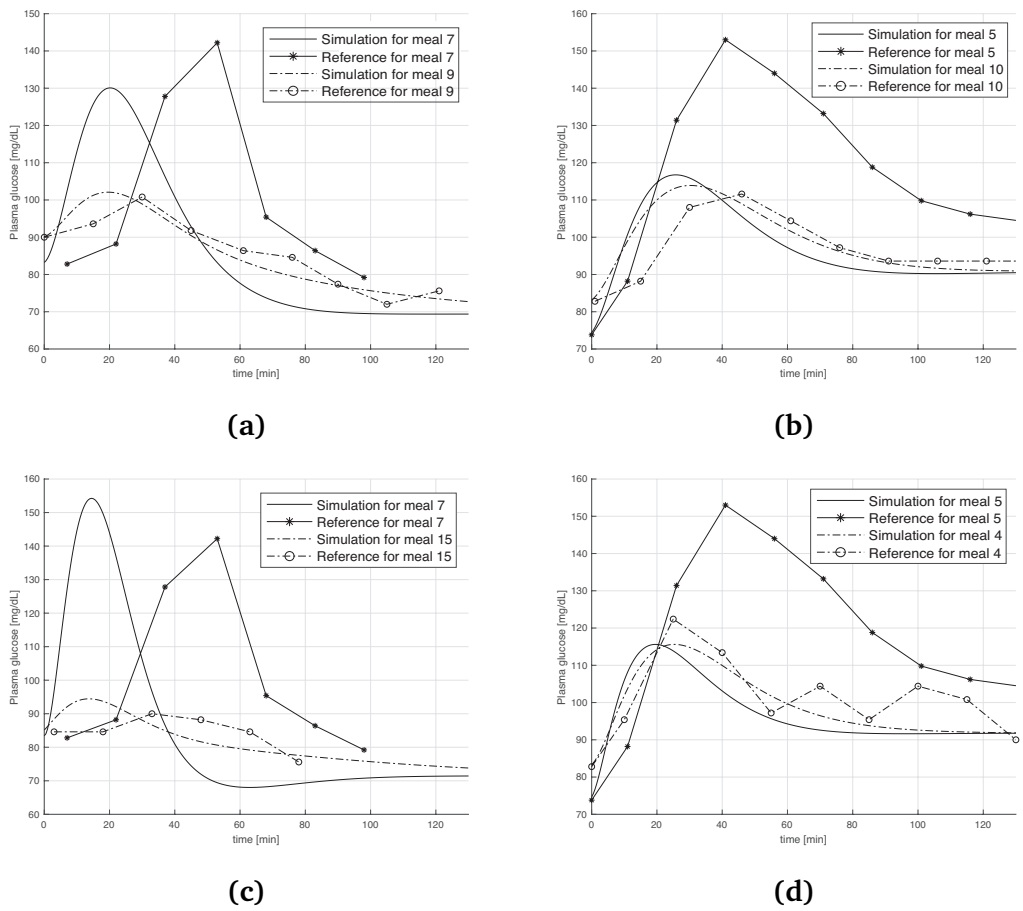

Figure 6.11: SOGMM model parameter estimation result for best and worst meal.
(a) Reference from subject 1 for meals 7 ($d = 0.0010$) and 9 ($d = 0.4146$), and simulated prediction after parameter estimation, with linear FPF relationship.
(b) Reference from subject 2 for meals 5 ($d = 0.0024$) and 10 ($d = 0.2628$), and simulated prediction after parameter estimation, with linear FPF relationship.
(c) Reference from subject 1 for meals 7 ($d = 0.0001$) and 15 ($d = 0.3220$), and simulated prediction after parameter estimation, with quadratic FPF relationship.
(d) Reference from subject 2 for meals 5 ($d = 0.0015$) and 4 ($d = 0.2376$), and simulated prediction after parameter estimation, with quadratic FPF relationship.

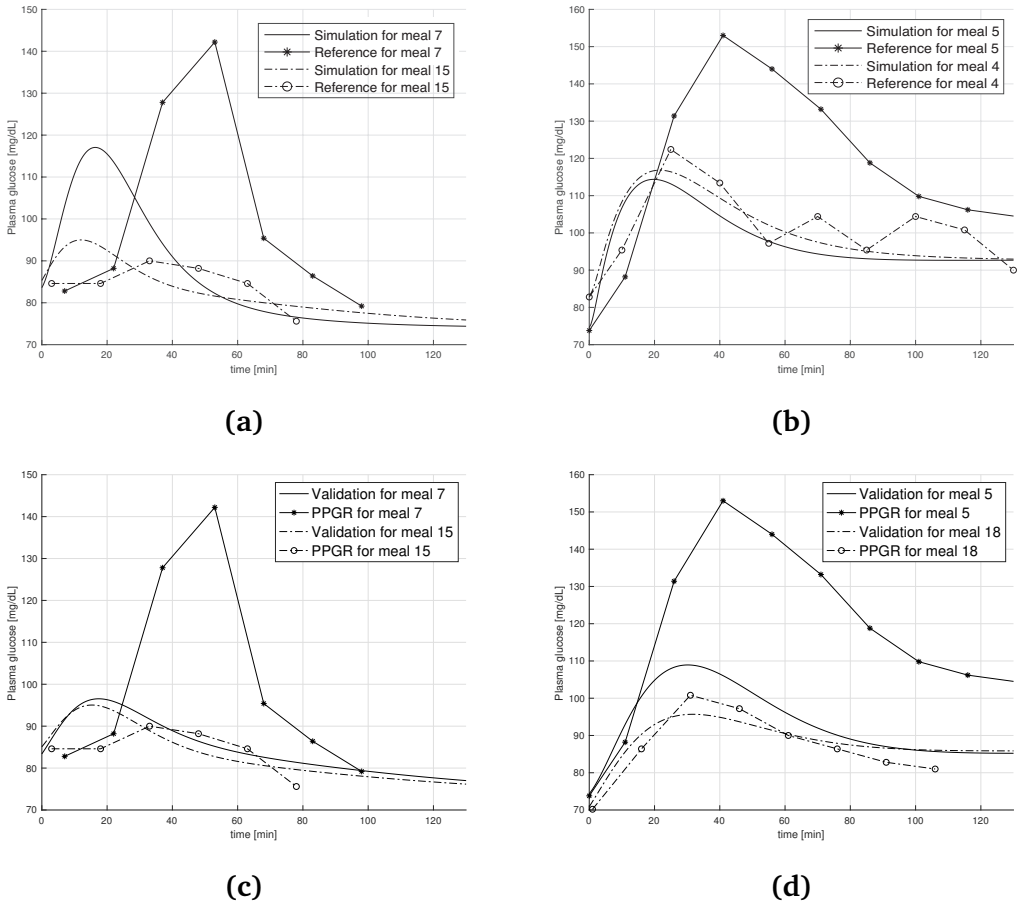

Figure 6.12: SOGMM model parameter estimation result for best and worst meal, for square root FPF relationship and no FPF relationship.
(a) Reference from subject 1 for meals 7 ($d = 0.0014$) and 15 ($d = 0.3272$), and simulated prediction after parameter estimation, with square root FPF relationship.
(b) Reference from subject 2 for meals 5 ($d = 0.0019$) and 4 ($d = 0.2094$), and simulated prediction after parameter estimation, with square root FPF relationship.
(c) Reference from subject 1 for meals 7 ($d = 0.0027$) and 15 ($d = 0.3434$), and simulated prediction after parameter estimation, with no FPF relationship.
(d) Reference from subject 2 for meals 5 ($d = 0.0012$) and 18 ($d = 0.4990$), and simulated prediction after parameter estimation, with no FPF relationship.

7 Discussion

7.1 Meal parameter estimation

Different ways of doing meal parameter estimation were presented in section 4.2. The problem at this moment in time is that the meal parameter estimation accuracy is not high enough for it to be used as an aid for people with diabetes, at least not for real life meals that are not from a specialized meal dataset.

A problem for the accuracy of the meal parameter estimations is that the variability in food preparation makes estimation and classification really hard. This is because two visually similar meals from two different images can have a very different macronutrient composition. Also, two not so visually similar meals can be very similar in macronutrient composition. This is a difficult problem that none of the current estimation techniques are able to solve, at least not without some amount of data for each case specifically.

Another problem is the runtime complexity of the models. Many of the presented applications can run on the smartphone, or is run on a remote server [58]. For future estimation techniques to obtain even better results, which is demanded if they are to be used by diabetic patients, the models will be even more complex. This will increase the runtime of the estimation, unless the current model architectures are utilized in an even more efficient manner.

For the augmented reality applications, the user interaction was reported to be one of the issues during testing. Not everyone have sufficient experience with a smartphone to be able to mark bounding boxes of the food on a touch screen. Also, mistakes can be made even for subjects with experience with a smartphone, if one is not familiar with the application. The applications should be used only by patients that have been using smartphones before.

In theory though, if the methods managed to classify the food correctly and estimate the amount accurately enough most or all of the time, they could have been used to get input for a glycemic prediction model. Then it would not be hard to obtain the macronutrient compositions of those meals, which again could have been used as input to a glycemic model. GI, on the other hand, is not as accessible for a given meal, so a classification algorithm would not have been able to find the GI for all meals. Therefore, if GI was a part of the input to a model, a meal classification method based on meal images would not have been sufficient to calculate the input.

7.2 PLSR analysis

In the PLSR analysis it was observed that for the subject 2 input with X as aCHO, fat, protein and fiber, fiber was the most important variable for prediction of iAUC. For the rest of the different meal info input, on the other hand, fiber was often one of the least important variables. A reason for this difference

could be the difference in macronutrient composition of the meals between Rozendaal, subject 1 and subject 2. For subject 1, the meals contained on average 1.23 times more aCHO than it contained fat, protein and fiber combined. For subject 2, this number was 0.56. A possible part of the explanation then might be that the amount of aCHO was low compared to the amount of fat, protein and fiber, and therefore fiber correlated more with the PPGR values.

Another reason could simply be the low amount of meals in the dataset. From subject 2 it was collected 20 meals. Since the PPGRs were collected in the daily life, even though the clearly disturbed measurements were taken out, it will not be the same as performing measurements in controlled environments. Daily life can and will have an impact one way or another, unless the subject is determined to sit still and wait until the PPGR has settled. Therefore, 20 meals might not be enough to catch the real correlations between meal info and the PPGRs, and at the same time exclude the non-significant disturbances. This could have lead to fiber having the highest correlation with the output, or this was just the true correlation.

In the PLSR results presented in figure 6.1 and table 6.1, the validation EV relative to the calibration EV was much higher for the Rozendaal data than for the subject 1 and 2 data. This might be surprising, considering the fact that the Rozendaal data is from many different subjects and study groups, while the subject 1 and subject 2 data are only from one person each, obviously. But the reason for this difference in EV might be explained by the difference in number of recorded meals. While the Rozendaal dataset collected contains 96 meals or OGTT, the subject 1 and subject 2 datasets contains 15 and 20 meals, respectively. Lower number of data gives fewer training data which might lead to a lower EV for the validation set in the cross validation.

7.3 Model parameter estimations

In the model parameter estimation, the parameters estimated for a single subject were quite similar for the estimations, for both the IVP and the SOGMM model. Also, the parameters that were lower for subject 1 than for subject 2 for one FPF relationship, generally tended to be lower for most of the others as well, and vice versa. This might indicate stability of the parameter estimations and the estimation algorithm, that the values were not fluctuating all over the range for the different estimations, but were fairly similar.

7.4 PPGR prediction

Overall, the glucose response predictions were most accurate using the original IVP and SOGMM models without any FPF input, but with added pancreatic insulin secretion. This contradicted the PLSR results, suggesting that fat, protein

and fiber could help explain the PPGR. One reason for this misfit could be that the models are not originally developed to include FPF input. This means that adding sensitivity for FPF input, might not necessarily give the model better prediction abilities. The prediction accuracy might have been better if the FPF relationships were modelled in another way, like with the FPF relationships described in equations (5.12)-(5.14) for IVP. Of the modelled FPF relationships, none of the three (linear, quadratic and square root) obtained significantly better results than the others. A possible explanation for this is that none of them was a particularly good way to model the effect of fat, protein and fiber on the glucose response.

As described earlier, the SOGMM model is more complex and has more state variables than the IVP model. Therefore it is more likely to catch the dynamics behind the glucose measurements than the IVP model will be. This, though, requires that the model is identifiable for the given model parameter set and plasma glucose data. The results showed that the SOGMM predictions were generally more accurate than the IVP model predictions. Also the parameter estimations were relatively consistent between the different model versions. These two things indicate that the SOGMM model parameters given in (6.2) were estimated fairly accurately for the given data.

For the SOGMM predictions the failure was often that PPGR curve was raising too early to fit the reference curve. This is especially visible in figure 6.11a, where the simulated curve for meal 7 has approximately the same height and length as the reference measurement for meal 7, but too early. The same phenomena can be observed for some of the other prediction/reference pairs in the other plots. The model clearly manages to mimic the dynamics behind the curve, but the response comes too early. The reason for this can simply be that the output of the model is plasma glucose concentration values, while the reference curve is measured subcutaneously, and with a CGM. CGMs have a time delay caused by both the transfer of glucose from plasma to the subcutaneous interstitial fluid, and the measurement averaging performed in the CGM [81]. Therefore, adding a state variable to the model representing the subcutaenous glucose concentration, could have given better predictions.

The glucose predictions for subject 1 were generally better than for subject 2. This is in agreement with the EVs found in the PLSR. Again, this can be related to the difference in macronutrient content of the meals for the two subjects, and of course a bigger variation in the responses that are not explained by macronutrient content, for subject 2.

The only model type for which the predictions were better for subject 2 than subject 1 were the ones not using FPF input. The subject 2 meals contained more fat, protein and fiber compared to carbohydrates, than the subject 1 meals did. This might explain why the exclusion of FPF from the model input gave very good predictions for the subject 2 data, compared to the models including FPF inputs. The high relative amount of fat, protein and fiber could have been

just a bad fit for the modelled FPF relationships.

Overall, the desirability values were not very high. For a perfect fit, which is not realistic to expect with real data input, the desirability value is 1. The best average desirability value obtained for the prediction here was 0.1882, which was for the subject 1 data, IVP model and no FPF input. This highlights how difficult it is to predict glucose responses accurately, and that such lower order models like the ones used here might be too simple to be able to predict real PPGRs.

7.5 Differences for healthy, DM1 and DM2

In this project, only healthy subjects and subject data were used. This will of course have had en effect on the result. Even though the overall goal with this is to be able to predict PPGRs for DM1 and DM2 patients, the task of analysing the macronutrient content's effect on the glucose response was maybe just as good to carry out on healthy data. This because glucose data from a DM1 or DM2 patient would in many cases be more variable, and the glucose dynamics affected by fat, protein and fiber would maybe have been harder to obtain.

On the other hand, to have performed the same analysis on DM1 and/or DM2 data, as well as the healthy data, would have given valuable information about fat, protein and fiber's effect on the PPGR in people with diabetes, and how it differs from the healthy FPF effect.

8 Conclusion

In this project, the modelling and prediction of postprandial glucose responses have been investigated. Especially, correlations between the macronutrient content of the meals and the glucose responses have been analysed.

The project contains a literature study, summarizing the different ways PPGR is explained and modelled. This shows that different meal/food parameters, like carbohydrates, GI, fat, protein and fiber have showed to have an effect on the glucose response after a meal. Also the metabolism model used is important for the accuracy of the prediction and what types of dynamics the prediction manages to recreate.

The second literature study focuses on meal recognition and classification with the use of a mobile phone camera and image classification algorithms. With the emergence of deep neural networks, general image classification and recognition have improved a lot the last couple of years. This also applies to meal images. Still, it is a long way to go before acceptable accuracies for the use of these in real life is achieved.

Glucose and meal data from Rozendaal et al. [1] and two additional subjects have been collected. The Rozendaal data was suboptimal to use, because indivudual recordings were not available, only study group averages, but the analysis did still contain valuable information.

PLSR analysis of said data was carried out, looking at the correlation between meal parameters and glucose response. The results were not surprising, as aCHO and GI looked to correlate positively with glucose response, and fat, protein and fiber correlated negatively, with fiber being less important than the others. This was the case for all data, except for subject 2, were fiber was the meal parameter with the highest prediction value in the PLSR model.

The Rozendaal data had the highest validation EV, and it is thought that this might originate from the much higher amount of glucose data than for subject 1 and 2. The Rozendaal data obtained an EV of between 40 and 50 $\%$ for both the calibration and validation analysis. The subject 1 and 2 data gained a highest calibration EV of 52.7% and 39.4%, respectively, while the validation EV were much lower. The sum of fat, protein and fiber was used as a meal parameter in the PLSR analysis, as well as the square and square root if it, obtaining reasonable results, fueling the idea of using it in the prediction models.

Two prediction models, IVP and SOGMM, were chosen to be used as prediction models, based on the low complexity, and thus higher model identifiability. A parameter sensitivity analysis was carried out, using input data from the collected datasets, obtaining two parameter sets suitable for parameters estimation.

Based on the chosen models and identifiable model parameter sets, parameter estimation and glucose response prediction was carried out. The models not including fat, protein and fiber as input got the best results, with the best

average desirability value of 0.1882, obtained with subject 1 data and the IVP model. Between the different ways of modelling the relationship between fat, protein and fiber, with the glucose response, none of them (linear, quadratic or square root) stood out as much better than the others. This could be because none of them was a good fit to the true relationship.

9 Suggestions for future work

DM1 and DM2 patients The same analysis could be carried out for DM1 and DM2 patients. Looking at how different kind of meal compositions affect DM1 and DM2 plasma glucose responses would be the next step. This is important because that is the people that will actually benefit from this research.

Different types of fat and proteins Just like carbohydrates, both fat and protein come in different forms. These different types may have different effects on digestion, and therefore also on the glucose response. Maybe, to get a better prediction result, how the different types of fat and proteins affect the glucose response should be taken into account.

Use amount of sugar as input A part of the explanation of how fast carbohydrates is digested is how much of it is sugar. Sugars are carbohydrates which will be digested faster than other carbohydrates, and will therefore raise the plasma glucose faster. If this is a part of the input, maybe predictions will be more accurate as well.

Different modelling of FPF input In this project, the sum of fat, protein and fiber, and the square and square root of the sum, was included in the model to affect how fast the carbohydrates were digested. This did not give a very good prediction result. A relationship between FPF and the glucose response was shown in the PLSR analysis, so there should be another way to model the relationship such that the predictions gets better because of it. This can be investigated further.

Estimate different model parameters One can not be sure that the model parameter set picked for estimation is really possible to estimate correctly. To try larger and smaller parameter sets to estimate could give an indication as to whether the parameter sets picked, and the sizes of them, were optimal or not.

Calculate insulin bolus based on predicted PPGR If an accurate glucose response calculator is developed, this can be used to decide the insulin bolus that should be injected. Further research could include some work regarding optimal insulin bolus calculation.

10 Bibliography

[1] Y. Rozendaal, A. Maas, C. Pul, W. J. Cottaar, H. Haak, P. Hilbers, and N. van Riel, "Model-based analysis of postprandial glycemic response dynamics for different types of food," *Clinical Nutrition Experimental*, 02 2018.

[2] P. M. Stige, *Implementation of a Metabolism Model for Insulin/Glucose Dynamics*. Trondheim, Norway: Norwegian University of Science and Technology, 2018, term project, Norwegian University of Science and Technology, Trondheim, Norway.

[3] I. D. Federation, "Idf diabetes atlas, eighth edition," 2017. [Online]. Available: http://www.diabetesatlas.org/

[4] J. Bass and J. Takahashi, "Circadian integration of metabolism and energetics," *Science (New York, N.Y.)*, vol. 330, pp. 1349–54, 12 2010.

[5] J. Yoshino, P. Almeda-Valdes, B. W Patterson, A. Okunade, S.-I. Imai, B. Mittendorfer, and S. Klein, "Diurnal variation in insulin sensitivity of glucose metabolism is associated with diurnal variations in whole-body and cellular fatty acid metabolism in metabolically normal women," *The Journal of clinical endocrinology and metabolism*, vol. 99, p. jc20141579, 05 2014.

[6] D. Zeevi, T. Korem, N. Zmora, D. Israeli, D. Rotshchild, A. Weinberger, O. Ben-Yacov, D. Lador, T. Avnit-Sagi, M. Lotan-Pompan, J. Suez, J. Mahdi, E. Matot, G. Malka, N. Kosower, M. Rein, G. Zilberman-Schapira, L. Dohnalová, M. Pevsner-Fischer, and E. Segal, "Personalized nutrition by prediction of glycemic responses," *Cell*, vol. 163, pp. 1079–1094, 11 2015.

[7] A.-S. Brazeau, H. Mircescu, K. Desjardins, C. Leroux, I. Strychar, J. Ekoé, and R. Rabasa-Lhoret, "Carbohydrate counting accuracy and blood glucose variability in adults with type 1 diabetes," *Diabetes research and clinical practice*, vol. 99, 11 2012.

[8] T. E Schap, B. Daugherty, E. Delp, D. Ebert, D. Kerr, and C. Boushey, "Adolescents in the united states can identify familiar foods at the time of consumption and when prompted with an image 14 h postprandial, but poorly estimate portions," *Public health nutrition*, vol. 14, pp. 1184–91, 02 2011.

[9] M. Andersson, "A comparison of nine pls1 algorithms," *Journal of Chemometrics*, vol. 23, pp. 518 – 529, 10 2009.

[10] R. Bergman, Y. Ider, C. Bowden, and C. Cobelli, "Quantitative estimation of insulin sensitivity," *The American journal of physiology*, vol. 236, pp. E667–77, 07 1979.

[11] C. Dalla Man, R. A. Rizza, and C. Cobelli, "Meal simulation model of the glucose-insulin system," *IEEE Transactions on Biomedical Engineering*, vol. 54, no. 10, pp. 1740–1749, Oct 2007.

[12] C. D. Man, F. Micheletto, D. Lv, M. Breton, B. Kovatchev, and C. Cobelli, "The uva/padova type 1 diabetes simulator: New features," *Journal of Diabetes Science and Technology*, vol. 8, no. 1, pp. 26–34, 2014, pMID: 24876534. [Online]. Available: https://doi.org/10.1177/1932296813514502

[13] J. A. Jacquez and T. Perry, "Parameter estimation: local identifiability of parameters," *American Journal of Physiology-Endocrinology and Metabolism*, vol. 258, no. 4, pp. E727–E736, 1990, pMID: 2333964. [Online]. Available: https://doi.org/10.1152/ajpendo.1990.258.4.E727

[14] H. Miao, X. Xia, A. Perelson, and H. Wu, "On identifiability of nonlinear ode models and applications in viral dynamics," *SIAM review. Society for Industrial and Applied Mathematics*, vol. 53, pp. 3–39, 01 2011.

[15] J. Garcia-Tirado, C. Zuluaga-Bedoya, and M. D. Breton, "Identifiability analysis of three control-oriented models for use in artificial pancreas systems," *Journal of Diabetes Science and Technology*, vol. 12, no. 5, pp. 937–952, 2018, pMID: 30095007. [Online]. Available: https://doi.org/10.1177/1932296818788873

[16] H. Stigter, D. Joubert, and J. Molenaar, "Observability of complex systems: Finding the gap," *Scientific Reports*, vol. 7, 11 2017.

[17] E. C. Harrington, "The desirability function," *Industrial Quality Control*, vol. 21, no. 10, pp. 494–498, 1965.

[18] S. N. Deming, "Multiple-criteria optimization," *Journal of Chromatography A*, vol. 550, pp. 15–25, 12 1991.

[19] G. Nicolaysen and P. Holck, *Kroppens funksjon og oppbygning*. Gyldendal Akademisk, 2013.

[20] "Evidence-based nutrition principles and recommendations for the treatment and prevention of diabetes and related complications,"

Diabetes Care, vol. 25, no. 1, pp. 202–212, 2002. [Online]. Available: http://care.diabetesjournals.org/content/25/1/202

[21] D. Jenkins, T. Wolever, R. Taylor, H. Barker, H. Fielden, J. Baldwin, A. Bowling, H. Newman, A. Jenkins, and D. Goff, "Glycemic index of foods: A physiological basis for carbohydrate exchange," *The American journal of clinical nutrition*, vol. 34, pp. 362–6, 04 1981.

[22] F. S. Atkinson, K. Foster-Powell, and J. C. Brand-Miller, "International tables of glycemic index and glycemic load values: 2008," *Diabetes Care*, vol. 31, no. 12, pp. 2281–2283, 2008. [Online]. Available: http://care.diabetesjournals.org/content/31/12/2281

[23] "Glycemic index, glycemic load and glycemic response: An international scientific consensus summit from the international carbohydrate quality consortium (icqc)." vol. 25, no. 9, pp. 795–815, 2015. [Online]. Available: http://dx.doi.org/10.1016/j.numecd.2015.05.005

[24] X. Lan-Pidhainy and T. M S Wolever, "Are the glycemic and insulinemic index values of carbohydrate foods similar in healthy control, hyperinsulinemic and type 2 diabetic patients?" *European journal of clinical nutrition*, vol. 65, pp. 727–34, 03 2011.

[25] A. G. Liu, M. M. Most, M. M. Brashear, W. D. Johnson, W. T. Cefalu, and F. L. Greenway, "Reducing the glycemic index or carbohydrate content of mixed meals reduces postprandial glycemia and insulinemia over the entire day but does not affect satiety," *Diabetes Care*, vol. 35, no. 8, pp. 1633–1637, 2012. [Online]. Available: http://care.diabetesjournals.org/content/35/8/1633

[26] J. Brand-Miller and A. Buyken, "The glycemic index issue," *Current opinion in lipidology*, vol. 23, pp. 62–7, 12 2011.

[27] C. B. Ebbeling, D. S. Ludwig, T. A. Wadden, and A. N. Fabricatore, "Continuous glucose monitoring to assess the ecologic validity of dietary glycemic index and glycemic load," *The American Journal of Clinical Nutrition*, vol. 94, no. 6, pp. 1519–1524, 11 2011. [Online]. Available: https://doi.org/10.3945/ajcn.111.020354

[28] J. Bao, F. Atkinson, P. Petocz, W. C. Willett, and J. C. Brand-Miller, "Prediction of postprandial glycemia and insulinemia in lean, young, healthy adults: glycemic load compared with carbohydrate content alone," *The American Journal of Clinical Nutrition*, vol. 93, no. 5, pp. 984–996, 2011. [Online]. Available: http://dx.doi.org/10.3945/ajcn.110.005033

[29] M. Thomas, V. Swan, Z. I. Ahmad, J. C. Brand-Miller, P. Petocz, and S. Colagiuri, "Physiological Validation of the Concept of Glycemic Load in Lean Young Adults," *The Journal of Nutrition*, vol. 133, no. 9, pp. 2728–2732, 09 2003. [Online]. Available: https://doi.org/10.1093/jn/133.9.2728

[30] S. M. Williams, B. J. Venn, T. Perry, R. Brown, A. Wallace, J. I. Mann, and T. J. Green, "Another approach to estimating the reliability of glycaemic index," *British Journal of Nutrition*, vol. 100, no. 2, pp. 364–372, 2008.

[31] A. P. Shukla, R. G. Iliescu, C. E. Thomas, and L. J. Aronne, "Food order has a significant impact on postprandial glucose and insulin levels," *Diabetes Care*, vol. 38, no. 7, pp. e98–e99, 2015. [Online]. Available: http://care.diabetesjournals.org/content/38/7/e98

[32] P. C. J. K. Henry, H. J. Lightowler, K. J. Newens, and N. Pata, "The influence of adding fats of varying saturation on the glycaemic response of white bread," *International Journal of Food Sciences and Nutrition*, vol. 59, no. 1, pp. 61–69, 2008. [Online]. Available: https://doi.org/10.1080/09637480701664183

[33] B. Owen and T. Wolever, "Effect of fat on glycaemic responses in normal subjects: A dose-response study," *Nutrition Research*, vol. 23, 10 2003.

[34] M. Lodefalk, J. Aman, and P. Bang, "Effects of fat supplementation on glycaemic response and gastric emptying in adolescents with type 1 diabetes," *Diabetic medicine : a journal of the British Diabetic Association*, vol. 25, pp. 1030–5, 09 2008.

[35] G. S Frost, A. Brynes, W. S Dhillo, S. R Bloom, and M. McBurney, "The effects of fiber enrichment of pasta and fat content on gastric emptying, glp-1, glucose, and insulin responses to a meal," *European journal of clinical nutrition*, vol. 57, pp. 293–8, 02 2003.

[36] T. Wolever and Y. Mullan, "Sugars and fat have different effects on postprandial glucose responses in normal and type 1 diabetic subjects," *Nutrition, metabolism, and cardiovascular diseases : NMCD*, vol. 21, pp. 719–25, 02 2011.

[37] F. Q. Nuttall, A. D. Mooradian, M. C. Gannon, C. Billington, and P. Krezowski, "Effect of protein ingestion on the glucose and insulin response to a standardized oral glucose load," *Diabetes Care*, vol. 7, no. 5, pp. 465–470, 1984. [Online]. Available: http://care.diabetesjournals.org/content/7/5/465

[38] A. Karamanlis, F. D. Bartholomeusz, J. M. Wishart, K. L. Jones, M. Bellon, M. Horowitz, R. Chaikomin, S. Doran, and C. K. Rayner, "Effects of protein on glycemic and incretin responses and gastric emptying after oral glucose in healthy subjects," *The American Journal of Clinical Nutrition*, vol. 86, no. 5, pp. 1364–1368, 11 2007. [Online]. Available: https://doi.org/10.1093/ajcn/86.5.1364

[39] U. Gunnerud, J. J. Holst, E. Östman, and I. Björck, "The glycemic, insulinemic and plasma amino acid responses to equi-carbohydrate milk meals, a pilot- study of bovine and human milk," *Nutrition Journal*, vol. 11, no. 1, p. 83, Oct 2012. [Online]. Available: https://doi.org/10.1186/1475-2891-11-83

[40] E. Moghaddam, J. A. Vogt, and T. M. S. Wolever, "The effects of fat and protein on glycemic responses in nondiabetic humans vary with waist circumference, fasting plasma insulin, and dietary fiber intake," *The Journal of Nutrition*, vol. 136, no. 10, pp. 2506–2511, 2006. [Online]. Available: http://dx.doi.org/10.1093/jn/136.10.2506

[41] A. Neu, F. Behret, R. Braun, S. Herrlich, F. Liebrich, M. Loesch-Binder, A. Schneider, and R. Schweizer, "Higher glucose concentrations following protein- and fat-rich meals - the tuebingen grill study: A pilot study in adolescents with type 1 diabetes," *Pediatric Diabetes*, vol. 16, 10 2014.

[42] R. A. Samra and G. H. Anderson, "Insoluble cereal fiber reduces appetite and short-term food intake and glycemic response to food consumed 75 min later by healthy men," *The American Journal of Clinical Nutrition*, vol. 86, no. 4, pp. 972–979, 10 2007. [Online]. Available: https://doi.org/10.1093/ajcn/86.4.972

[43] D. J. Jenkins, T. M. Wolever, A. R. Leeds, M. A. Gassull, P. Haisman, J. Dilawari, D. V. Goff, G. L. Metz, and K. G. Alberti, "Dietary fibres, fibre analogues, and glucose tolerance: importance of viscosity." *BMJ*, vol. 1, no. 6124, pp. 1392–1394, 1978. [Online]. Available: https://www.bmj.com/content/1/6124/1392

[44] S. Holt, R. C Heading, D. C Carter, L. F Prescott, and P. Tothill, "Effect of gel fibre on gastric emptying and absorption of glucose and paracetamol," *Lancet*, vol. 1, pp. 636–9, 04 1979.

[45] A. H. Maas, Y. J. W. Rozendaal, C. van Pul, P. A. J. Hilbers, W. J. Cottaar, H. R. Haak, and N. A. W. van Riel, "A physiology-based model describing heterogeneity in glucose metabolism: The core of the eindhoven diabetes education simulator (e-des)," *Journal of Diabetes Science and Technology*,

vol. 9, no. 2, pp. 282–292, 2015, pMID: 25526760. [Online]. Available: https://doi.org/10.1177/1932296814562607

[46] S. S. Kanderian, S. Weinzimer, G. Voskanyan, and G. M. Steil, "Identification of intraday metabolic profiles during closed-loop glucose control in individuals with type 1 diabetes," *Journal of Diabetes Science and Technology*, vol. 3, no. 5, pp. 1047–1057, 2009, pMID: 20144418. [Online]. Available: https://doi.org/10.1177/193229680900300508

[47] S. S. Kanderian, S. A. Weinzimer, and G. M. Steil, "The identifiable virtual patient model: Comparison of simulation and clinical closed-loop study results," *Journal of Diabetes Science and Technology*, vol. 6, no. 2, pp. 371–379, 2012, pMID: 22538149. [Online]. Available: https://doi.org/10.1177/193229681200600223

[48] G. Shapira, O. Yodfat, A. HaCohen, P. Feigin, and R. Rubin, "Bolus guide: A novel insulin bolus dosing decision support tool based on selection of carbohydrate ranges," *Journal of Diabetes Science and Technology*, vol. 4, no. 4, pp. 893–902, 2010, pMID: 20663453. [Online]. Available: https://doi.org/10.1177/193229681000400418

[49] F. K. Bishop, D. M. Maahs, G. Spiegel, D. Owen, G. J. Klingensmith, A. Bortsov, J. Thomas, and E. J. Mayer-Davis, "The carbohydrate counting in adolescents with type 1 diabetes (ccat) study," *Diabetes Spectrum*, vol. 22, no. 1, pp. 56–62, 2009. [Online]. Available: http://spectrum.diabetesjournals.org/content/22/1/56

[50] L. T. Meade and W. E. Rushton, "Accuracy of carbohydrate counting in adults," *Clinical Diabetes*, vol. 34, no. 3, pp. 142–147, 2016. [Online]. Available: http://clinical.diabetesjournals.org/content/34/3/142

[51] A. Myers, N. Johnston, V. Rathod, A. Korattikara, A. Gorban, N. Silberman, S. Guadarrama, G. Papandreou, J. Huang, and K. Murphy, "Im2calories: Towards an automated mobile vision food diary," pp. 1233–1241, Dec 2015.

[52] V. Bettadapura, E. Thomaz, A. Parnami, G. Abowd, and I. Essa, "Leveraging context to support automated food recognition in restaurants," 10 2015.

[53] J. Dehais, M. Anthimopoulos, and S. Mougiakakou, "Food image segmentation for dietary assessment," in *Proceedings of the 2Nd International Workshop on Multimedia Assisted Dietary Management*, ser. MADiMa '16. New York, NY, USA: ACM, 2016, pp. 23–28. [Online]. Available: http://doi.acm.org/10.1145/2986035.2986047

[54] "Food-101 – mining discriminative components with random forests," https://www.vision.ee.ethz.ch/datasets_extra/food-101/, accessed 2019-04-12.

[55] "Foodcam - uec food 100 and uec food 256," http://foodcam.mobi/dataset.html, accessed 2019-04-12.

[56] M. M. Anthimopoulos, L. Gianola, L. Scarnato, P. Diem, and S. G. Mougiakakou, "A food recognition system for diabetic patients based on an optimized bag-of-features model," *IEEE Journal of Biomedical and Health Informatics*, vol. 18, no. 4, pp. 1261–1271, July 2014.

[57] Sivic and Zisserman, "Video google: a text retrieval approach to object matching in videos," pp. 1470–1477 vol.2, Oct 2003.

[58] C. Liu, Y. Cao, Y. Luo, G. Chen, V. Vokkarane, M. Yunsheng, S. Chen, and P. Hou, "A new deep learning-based food recognition system for dietary assessment on an edge computing service infrastructure," *IEEE Transactions on Services Computing*, vol. 11, no. 2, pp. 249–261, March 2018.

[59] "Imagenet," http://www.image-net.org, accessed 2019-04-12.

[60] Y. Kawano and K. Yanai, "Foodcam: A real-time mobile food recognition system employing fisher vector," 01 2014, pp. 369–373.

[61] K. Yanai and Y. Kawano, "Food image recognition using deep convolutional network with pre-training and fine-tuning," in *2015 IEEE International Conference on Multimedia Expo Workshops (ICMEW)*, June 2015, pp. 1–6.

[62] R. Tanno, K. Okamoto, and K. Yanai, "Deepfoodcam: A dcnn-based real-time mobile food recognition system," 10 2016, pp. 89–89.

[63] H. Hassannejad, G. Matrella, P. Ciampolini, I. De Munari, M. Mordonini, and S. Cagnoni, "Food image recognition using very deep convolutional networks," in *Proceedings of the 2Nd International Workshop on Multimedia Assisted Dietary Management*, ser. MADiMa '16. New York, NY, USA: ACM, 2016, pp. 41–49. [Online]. Available: http://doi.acm.org/10.1145/2986035.2986042

[64] C. Szegedy, V. Vanhoucke, S. Ioffe, J. Shlens, and Z. Wojna, "Rethinking the inception architecture for computer vision," *2016 IEEE Conference on Computer Vision and Pattern Recognition (CVPR)*, pp. 2818–2826, 2016.

[65] M. Bolaños and P. Radeva, "Simultaneous food localization and recognition," in *2016 23rd International Conference on Pattern Recognition (ICPR)*, Dec 2016, pp. 3140–3145.

[66] T. Stütz, R. Dinic, M. Domhardt, and S. Ginzinger, "Can mobile augmented reality systems assist in portion estimation? a user study," pp. 51–57, Sep. 2014.

[67] M. Domhardt, M. Tiefengrabner, R. Dinic, U. Fötschl, G. J. Oostingh, T. Stütz, L. Stechemesser, R. Weitgasser, and S. W. Ginzinger, "Training of carbohydrate estimation for people with diabetes using mobile augmented reality," *Journal of Diabetes Science and Technology*, vol. 9, no. 3, pp. 516–524, 2015, pMID: 25883165. [Online]. Available: https://doi.org/10.1177/1932296815578880

[68] R. Dinic, M. Domhardt, S. Ginzinger, and T. Stütz, "Eatar tango: Portion estimation on mobile devices with a depth sensor," in *Proceedings of the 19th International Conference on Human-Computer Interaction with Mobile Devices and Services*, ser. MobileHCI '17. New York, NY, USA: ACM, 2017, pp. 46:1–46:7. [Online]. Available: http://doi.acm.org/10.1145/3098279.3125434

[69] R. Dinic and T. Stütz, "Eatar tango: Results on the accuracy of portion estimation," in *2017 IEEE International Symposium on Mixed and Augmented Reality (ISMAR-Adjunct)*, Oct 2017, pp. 284–287.

[70] S. K. R. M. F. Z. E. J. D. C. J. B. D. S. E. Junghoon Chae, Insoo Woo, "Volume estimation using food specific shape templates in mobile image-based dietary assessment," vol. 7873, 2011. [Online]. Available: https://doi.org/10.1117/12.876669

[71] S. Fang, F. Zhu, C. Jiang, S. Zhang, C. J. Boushey, and E. J. Delp, "A comparison of food portion size estimation using geometric models and depth images," in *2016 IEEE International Conference on Image Processing (ICIP)*, Sep. 2016, pp. 26–30.

[72] M. A. Subhi, S. H. Md. Ali, A. G. Ismail, and M. Othman, "Food volume estimation based on stereo image analysis," *IEEE Instrumentation Measurement Magazine*, vol. 21, no. 6, pp. 36–43, December 2018.

[73] M. Anthimopoulos, J. Dehais, S. Shevchik, B. H. Ransford, D. Duke, P. Diem, and S. Mougiakakou, "Computer vision-based carbohydrate estimation for type 1 patients with diabetes using smartphones," *Journal of Diabetes Science and Technology*, vol. 9, no. 3, pp. 507–515, 2015, pMID: 25883163. [Online]. Available: https://doi.org/10.1177/1932296815580159

[74] F. Libre, "The freestyle libre system," 2019. [Online]. Available: https://www.freestylelibre.co.uk/libre/products.html

[75] "Freestyle auto-assist neo software," https://freestylediabetes.co.uk/our-products/software/freestyle-auto-assist-neo-software, accessed 2019-05-15.

[76] "Lifesum health app," https://lifesum.com/, accessed 2019-05-15.

[77] "Matvaretabellen," https://www.matvaretabellen.no/, accessed 2019-05-15.

[78] C. S. AS, "Unscrambler - camo analytics," 2019. [Online]. Available: https://www.camo.com/unscrambler

[79] H. Wold, "Soft modelling by latent variables: The non-linear iterative partial least squares (nipals) approach," *Journal of Applied Probability*, vol. 12, no. S1, p. 117–142, 1975.

[80] F. Lindgren, P. Geladi, and S. Wold, "The kernel algorithm for pls," *Journal of Chemometrics*, vol. 7, pp. 45 – 59, 01 1993.

[81] G. Schmelzeisen-Redeker, M. Schoemaker, H. Kirchsteiger, G. Freckmann, L. Heinemann, and L. Del Re, "Time delay of cgm sensors: Relevance, causes, and countermeasures," *Journal of diabetes science and technology*, vol. 9, 08 2015.

Appendix A

Appendix A.1 Data collected from Rozendaal et al.

Publication	Meal	Carbs [g	aCHO	Fat [g]	Protein [	Fiber [g]	GI	0	15	30	45	60	90	120
Anderwald et al	glucose (male)	75	75	0	0	0	100	5,05	6,58	8,15	7,87	6,94	5,63	5,15
	glucose (female)	75	75	0	0	0	100	4,94	6,3	7,29	7,24	6,97	5,85	5,63
Backhouse et al	medium GI breakfast	152	136	3	18	16	51	4,9	6,22	5,31		5,36		4,91
	high GI breakfast	123	121	2	16	2	77	4,9	6,63	5,54		5,24		4,55
Bondia-Pons et al	white bread	53,7	50	4,5	9,3	3,7	53	5	5,86	7,04	6,34	5,38	4,27	4,69
	sourdough rye bread	57,6	50	0,9	5,4	7,6	70	5	5,74	6,54	5,92	5,38	4,72	4,75
Brown et al	glucose	75	75	0	0	0	100	4,5	6,28	7,25	7,04	6,48	6,49	6,02
Ceriello et al	glucose	75	75	0	0	0	100	4,8		6,22		7,38	6,81	5,05
Christiansen et al	glucose	75	75	0	0	0	100	4,5	6,79	8,17	7,51	6,51	5,57	3,99
Cocate et al	high GI breakfast	136,6	87,46	6,83	11,78	49,14	79	4,72		6,83		5,36	4,94	
	low GI breakfast	148,24	80,38	7,42	12,78	67,86	28	4,72		4,83		4,53	4,63	
Duvivier et al	glucose (sitting)	75	75	0	0	0	100	4,6	5,91	7,03	7,15	6,18	5,71	5,09
	glucose (exercise)	75	75	0	0	0	100	4,5	6,09	7,65	7,62	6,85	6,03	5,12
	glucose(min. int. phys. act.)	75	75	0	0	0	100	4,5	5,94	7,26	7,62	6,91	5,88	5,35
Gunnerud et al	white bread	26,7	25	2,5	3,7	1,7	70	4,4	4,93	6,07	6,17	5,31	4,73	4,66
	bovine milk	25	25	7,6	16,8	0	30	4,4	4,62	5,68	4,97	4,35	4,24	4,34
	casein drink	25	25	7,7	16,8	0	30	4,4	4,54	5,42	4,8	4,14	4,28	4,35
	human milk	25	25	5,7	3,5	0	40	4,4	5,03	5,92	5,28	4,04	4,13	4,41
	whey drink	25	25	7,4	16,2	0	42	4,4	4,7	5,65	4,99	4,14	4,64	4,69
Hare et al	glucose	50	50	0	0	0	100	5	6,71	8,97	9,15	8,77	5,86	4,31
Henry et al	Potato	54,9	50	4	6	4,9	93	5	5,99	8,5	8,6	8,27	6,11	4,72
	Pasta	56,1	50	4	8	6,1	61	5	5,66	6,82	6,18	5,54	5,49	5,7
	White toast	52,54	50	2	9	2,54	50	5	5,56	6,85	6,95	6,5	5,29	5,17
Hätönen et al.	glucose	50	50	0	0	0	100	4,9	6,53	6,9	6,38	5,79	5,08	4,51
	white bread	53,4	50	2,2	8,5	3,4	70	4,9	5,81	6,73	6,24	5,64	5,05	4,95
	rye bread	63,6	50	2,2	10,3	13,6	78	4,9	5,81	6,56	6,34	5,65	5,19	5,09
	oatmeal porridge	60,9	50	6,4	13,4	10,9	76	4,9	6,13	6,8	5,97	5,33	5	4,74
	mashed potato	57,4	50	15,9	6,3	7,4	92	4,9	6,18	6,8	5,97	5,47	4,74	4,39
Ivović et al.	glucose	75	75	0	0	0	100	4,72		7,51		7,19	6,24	5,64
Jenkins et al	cornflakes with milk	58	56	2,4	10	2	79	5	5,79	7,76	8,31	7,4	5,76	4,97
	jasmin rice	50	50	0	4,2	0	70	5	6,11	7,85	7,68	6,96	6,34	5,16
	strawberry yoghurt	50	50	4	8	0	47	5	6,22	7,64	6,5	5,25	4,48	4,35
Juntunen et al	white bread	53,1	50	3	8,4	3,1	70	5,2	5,6	6,89	6,26	5,73	5,11	4,93
	whole-kernel rye bread	62,8	50	2,6	7,4	12,8	57	5,2	5,7	6,64	6,3	5,82	5,21	5,19
	beta-glucan rye bread	67,1	50	2,4	10,5	17,1	66	5,2	5,79	6,84	6,17	5,57	5,24	5,27
	whole meal pasta	55,6	50	4,7	12,1	5,6	58	5,2	5,57	6,26	5,86	5,48	5,33	5,34
Keogh et al	barley lunch	94	79,5	28	25	14,5	49	5		6,64		6,61		5,68
	wheat lunch	102	96,2	26	23	5,8	61	5		6,76		7,65		6,28
	white bread with jam	56	53,7	9,1	7,1	2,3	65	5	6,03	7,14	6,85	5,92	5,52	5,31
	Burgen bread with jam	45,5	36,9	13,2	11,3	8,6	42	5	6,05	6,92	6,07	5,15	5,04	5,03
Larsen et al	glucose	75	75	0	0	0	100	5,4		7,76		6,72	5,73	5,33
Leeman et al	french fries	37,22	32,5	10,3	5,1	4,72	54	5	5,62	5,99	6,24	5,43		4,79
	boiled potatoes	55,18	50,3	0,9	6,7	4,88	78	5	6,24	7,19	8,01	6,96		
	mashed potatoes	50	46,2	3,5	5,9	3,8	87	5	6,25	7,41	8,51	7,18		
	mashed potatoes	50	46,2	3,5	5,9	3,8	87	5	6,59	7,42	7,89	6,53		
	white bread	53,7	50	4,2	10,3	3,7	70	5	5,59	6,61	7,86	7,03		
	french fries	57,72	50	15,4	4,8	7,72	54	5	5,51	6,3	7,22	6,36		5,63
	boiled potatoes	54,88	50	0,1	1,6	4,88	78	5	5,95	7,04	8,19	7,63		
	boiled potatoes with sunflow	54,88	50	15,4	1,6	4,88	92	5	6,03	7,03	8,03	7,05		
Lott et al	glucose	75	75	0	0	0	100	4,88		6,66		5,88	5,61	5,83
Matsuda et al	glucose	75	75	0	0	0	100	5,16		7,75		7,67	6,86	6,45
Miller et al	glucose	50	50	0	0	0	100	4,61	6,22	7,44	7,11	6,22	5	4,72
	SmartZone bar	58,33	50	19,44	44,44	8,33	11	4,72	5,22	4,77	4,33	4,22	4,33	4,61
Miyazaki et al.	glucose	75	75	0	0	0	100	4,9		8,6		5,9		4,3
Moore et al.	glucose	75	75	0	0	0	100	4,8	6,32	8,89	8,9	8,5	7,59	6,99
Muscelli et al.	glucose	75	75	0	0	0	100	5,5	6,75	7,89	7,64	7,34	6,64	6,37
Münstedt et al.	glucose	75	75	0	0	0	100	4,94	6,42	7,96	6,93	6,15	5,34	5,01
Nagai et al.	glucose	75	75	0	0	0	100	5,05		6,69		7,61	7,29	6,12
Nazare et al	high GI breakfast	66,7	65,1	12,4	12,7	1,6	66	5,31	5,6	7,18	7,48	6,94	6,3	6,24
	low GI breakfast	66,7	65,1	12,7	12,8	1,6	47	5,15	5,4	6,48	6,72	6,3	5,66	5,66
Numao et al.	glucose	75	75	0	0	0	100	5,1	6,42	7,1	7,05	6,69	6,08	5,43
Ozeki et al.	glucose	75	75	0	0	0	100	5,02		8,89		8,2		6,08
Pamidi et al.	glucose	75	75	0	0	0	100	5		7,89		7,6	6,55	5,78
Penesová et al.	glucose	75	75	0	0	0	100	4,7	6,61	7,99	8,63	8,81	7,93	7,12
Priebe et al	glucose	50	50	0	0	0	100	5,1	6,99	8,28	7,97	7,66	6,02	4,88
	wholemeal wheat bread	64,6	50	2,1	11,5	14,6	74	4,9	6,67	7,01	6,02	5,09	4,93	4,57
Ranawana et al	basmati rice	77,6	77,2	0,4	8,6	0,4	57	4,4	5,09	6,25	5,82	5,34	4,73	4,63
	spaghetti	73	70,4	1,4	12,5	2,6	49	4,4	4,82	5,49	5,01	4,79	4,62	4,5

Figure Appendix A.1: Data collected from Rozendaal et al. (Part 1)

Publication	Meal	Carbs [g	aCHO	Fat [g]	Protein [	Fiber [g]	GI	0	15	30	45	60	90	120
Reynolds et al	high GI breakfast	47,4	41,9	10,5	10,9	5,5	73	5,3		7,1		5,34		4,38
	low GI breakfast	46,7	41	11,2	10,4	5,7	37	5,1		6,52		4,81		4,67
	high GI snack	30,9	26,6	6,8	6,9	4,3	74	5		6,22		5,92		5,23
	low GI snack	30,5	25,8	7,4	6	4,7	44	5		5,54		5,68		4,98
	high GI lunch	62,1	53,4	15,3	16,1	8,7	84	5,2		7,64		7,09		4,83
	low GI lunch	61,8	52,5	14,5	16,8	9,3	48	5		6,17		5,13		5,5
	high GI dinner	83,8	73,6	18,9	22,8	10,2	89	5		6,63		6,12		
	low GI dinner	84,9	74,6	18,9	23,1	10,3	39	5,2		5,67		6,05		
Rosario et al	glucose	75	75	0	0	0	100	4,1		6,35		6,1	5,49	5,4
Solomon et al	glucose	75	75	0	0	0	100	4,99		7,46		5,79	4,73	4,18
Suzuki et al	glucose	75	75	0	0	0	100	4,65		6,83		6,07		5,05
Wachters-Hagedoorn et al.	glucose	50	50	0	0	0	100	5,3	7,13	8,47	8,12	7,28	5,74	4,68
	cornstarch	50,5	50	0	0,1	0,5	70	5,2	5,92	6,14	6,04	6,03	5,86	5,93
	corn pasta	38,2	32,7	1	3,8	5,5	73	5,3	6,2	6,31	6,06	5,67	5,36	5,33
Wolever et al.	glucose	50	50	0	0	0	100	4,8	6,43	7,66	7,3	6,35	5,01	4,23
	fibre and fruit cereal meal	60,39	50,1	2,6	10,2	10,29	65	4,8	6,51	7,96	6,8	5,56	5,01	4,99
	high-fibre cereal meal	53	41,9	2,5	11,1	11,1	35	4,8	5,95	7,18	6,03	5,28	5,17	5,16
	omelette with whole-meal br	28,32	20,2	9,6	17,5	8,12	66	4,8	5,21	6,17	5,76	5,24	5,01	4,95
	omelette with honey and oat	26,65	15,5	10,3	17,1	11,15	40	4,8	5,18	5,95	5,65	5,26	5	5
	whole-wheat cereal meal	50,62	46,7	1,5	6,9	3,92	55	4,8	6,94	7,97	6,62	5,32	5,01	5
	cornflakes and wholewheat l	78,2	71,9	11,9	11,4	6,3	68	4,4	6,08	7,24	6,4	5,54	5,04	4,64
	twelve-grain bagel	74,4	69,4	11,2	13,3	5	67	4,4	5,85	7,07	5,97	5,38	5,01	5
	whole-rye pumpernickel, cra	78,93	69,6	13,7	11,2	9,33	51	4,4	6,57	7,01	6,17	5,34	4,81	4,81
	whole-rye pumpernickel, stra	82,92	79,4	12,2	6	3,52	44	4,4	5,66	6,72	6,36	5,63	5,14	4,84
	egg, french fries and wholew	41,4	37,9	18,2	16,7	3,5	67	4,4	5,43	6,57	5,72	4,74	4,36	4,32
	bran muffin	44,26	41,4	9,7	5	2,86	58	4,4	5,51	6,4	5,48	5,03	4,72	4,54
	strawberry yoghurt, fruit	58,26	57	8	5,3	1,26	42	4,4	5,3	6,21	5,4	4,79	4,5	4,36
Yamauchi et al.	glucose	75	75	0	0	0	100	4,66		7,4		6,17		5,09

Figure Appendix A.2: Data collected from Rozendaal et al. (Part 2)

Appendix A.2 Glucose measurements and meal info

Måltid	Klokkeslett	aCHO	Fat	Protein	Fiber	Målinger	Column1	Column2	Column3	Column4	Column5	Column6	Column7	Column8
Frokost1704	07:20	70,68	9,3	21,4	8,42	0	15	30	45	60	75	90		
						4,30	4,80	5,60	5,20	4,60	4,80	5,00		
Middag1704	21:05	132,22	19,3	52,1	5,68	2	17	32	47	62	77	92	107	122
						3,9	4,6	7,1	7,6	6,4	5,6	5,6	5,1	4,3
Middag1904	18:22	142,58	14,8	34,9	17,32	-3	12	27	42	57	72	87	102	117
						4,2	5,1	6,1	6,3	5,7	4,6	4	4,1	4,1
Frokost2004	09:42	129,13	23,3	43,4	32,77	-5	10	25	41	56	71	86	101	116
						4,1	4,6	5,7	6,3	5,2	4,7	4,6	4,3	4,6
Frokost2104	10:38	76	17,7	29,6	22,5	-8	7	21	36	51	66	82	97	
						4,4	4,2	4,9	6,3	5,8	4,1	3,6	4,1	
MM2104	19:20	40,02	8,5	4,3	5,78	-4	11	27	42	57	72			
						4,5	4,9	6,1	6,3	5,5	4,9			
Kveldsmat2104	21:55	61,3	16,9	4,6	0	7	22	37	53	68	83	98		
						4,6	4,9	7,1	7,9	5,3	4,8	4,4		
Frokost2204	09:55	48	20,2	25,4	12,6	-5	10	25	40	55	71			
						4,1	4,2	4,3	4,6	4,9	4,3			
Lunsj2204	13:06	57,6	15,3	17,7	9,7	0	15	30	45	61	76	90	105	121
						5	5,2	5,6	5,1	4,8	4,7	4,3	4	4,2
Frokost2304	07:49	61,59	11,9	17,1	8,31	7	22	37	52	67				
						4,3	4,7	5,2	4,6	4,4				
Lunsj2304_1	11:56	43,1	19,5	26,8	16,5	1	16	31	46	61	76	91	107	122
						4,3	4,1	5,1	5,3	5,1	4,6	4,2	3,9	3,9
Lunsj2304_2	14:20	43,1	19,5	26,8	16,5	8	23	38	53	68	83	98	113	
						4,5	4,9	5,4	5,1	4,4	4,2	4,7	4,7	
Middag2304	17:53	69,64	36,5	50,5	6,96	6	20	35	51	66	81	96	111	
						4,2	5	5,4	4,3	4,1	4,4	4,1	4,1	
Lunsj2404_1	11:05	46,8	17,9	21	16,5	-2	13	28	43	58	73			
						3,8	4	4,8	4,9	3,8	3,6			
Lunsj2404_2	14:01	43,1	19,5	26,8	16,5	3	18	33	48	63	78			
						4,7	4,7	5	4,9	4,7	4,2			

Figure Appendix A.3: Meal info and glucose for subject 1
Meal info displayed on the left part of the table. The corresponding glucose measurement times and values are displayed over two rows for every meal on the right side.

Måltid	Klokkeslett	aCHO	Fat	Protein	Fiber	Målinger	Column1	Column2	Column3	Column4	Column5	Column6	Column7	Column8	Column9	Column10	Column11	Column12
Lunsj3004	11:37	43	6	9	5	-7	8	23	38	52	68	83	98	113				
						4.7	5.2	5.9	6.9	7.2	6.3	5.4	4.8	4.4				
Middag3004	18:47	19	2	26	6	-2	14	28	43	58	74	89	104	119				
						4.6	5.5	7.8	7.7	7	6.3	5.9	5.5	5.3				
Frokost0105	09:00	9	27	21	7	3	18	34	48	63	78	93						
						4.9	6.2	7.4	6.8	5.6	4.3	4.1						
Lunsj0105	12:24	25	2	50	2	-5	10	25	40	55	70	85	100	115	130	145	160	175
						4.6	5.3	6.8	6.3	5.4	5.8	5.3	5.8	5.6	5	4.9	5.1	4.9
Middag0105	17:24	19	2	26	6	-5	11	26	41	56	71	86	101	116	131	146	161	176
						4.1	4.9	7.3	8.5	8	7.4	6.6	6.1	5.9	5.8	5.6	5.3	5.1
Frokost0205	06:25	11	12	22	0	3	18	33	48	63	78	93	108					
						4.6	5.4	6.2	6.3	5.8	5.1	4.4	4.4					
Lunsj0205	10:41	4	30	23	8	-4	12	27	42	57	72	87	102	117	132	147		
						4.5	4.7	5.3	6.1	6.3	5.9	5.4	5.1	5.1	4.9	4.8		
Middag0205	16:11	9	20	35	3	-2	13	28	43	58	73	88						
						4.6	5.1	6.3	6.7	6.7	6.4	5.6						
Frokost0305	08:45	4	0	12	1	-3	12	27	42	57	72	87	102					
						4.1	4.4	4.9	5.1	4.8	4.8	4.6	4.5					
Lunsj0305	15:12	21	14	39	1	1	15	30	46	61	76	91	106	121	136	151	166	181
						4.6	4.9	6	6.2	5.8	5.4	5.2	5.2	5.2	5.2	5.3	5.2	5
Frokost0405	06:15	18	2	7	1	0	16	31	46	61	76	91	106					
						4.2	5.4	6.6	6.1	5.3	5.1	4.8	4.7					
Lunsj0405	11:32	3	1	27	3	-1	14	29	44	59	74	89	104	119	134			
						4.8	5.2	6.4	6.6	6.2	5.8	5.6	5.4	5.1	4.8			
Middag0405	18:27	9	22	19	0	5	20	35	50	65	80	95	110	125	140			
						4.2	4.5	5	5.2	4.9	4.8	4.8	5	4.8	4.6			
Kveldsmat0405	20:57	17	32	5	0	5	20	35	50	65	80	95	110	125				
						4.8	5.3	6.1	6.1	5.8	5.7	5.4	4.9	4.4				
Lunsj0505	13:15	5	0	12	0	5	20	36	51	66	81	96	111	126				
						4.8	5.1	5.4	5.1	4.8	4.9	4.7	4.5	4.3				
Frokost0605	10:16	23	3	8	4	-6	8	23	38	53	68	83						
						4	4.4	6.1	7.7	7.3	5.6	4.7						
Middag0605	17:37	52	1	26	1	4	19	34	49	64								
						4.6	6.3	7.4	6.3	4.8								
Frokost0705	06:12	6	0	16	0	1	16	31	46	61	76	91	106					
						3.9	4.8	5.6	5.4	5	4.8	4.6	4.5					
Middag0705	15:35	28	17	25	3	-6	9	24	39	54	69	84	99	115	130	145		
						3.9	4.1	4.6	5.5	6.2	6.3	6.1	6.1	5.8	5.1	4.5		
Lunsj0805	14:03	65	25	22	2	0	15	30	45	60	75	90	105	120	135	150		
						5.2	7.1	7.8	8.4	8.4	7	5.7	5.6	5.4	5.1	4.8		

Figure Appendix A.4: Meal info and glucose for subject 2
Meal info displayed on the left part of the table. The corresponding glucose measurement times and values are displayed over two rows for every meal on the right side.

Appendix A.3

Parameter	Unit	Value	Min	Max
t_1	min	70.5	30	150
t_2	min	44.7	5.0	90
C_I	ml/min	1267	400	2200
p_2	1/min	0.0113	0.008	0.024
S_I	ml/μU	0.00152	0.0005	0.01
$GEZI$	1/min	0.0035	0.0	0.01
EGP	(mg/dl)/min	0.947	0.5	3.5
V_g	dl	213.9	fixed	
k_1	(μU dl)/(ml mg)	0.5	0.0	1.0
k_2	(μU dl)/(ml mg min)	0.00131	0.0	0.005
p_m	min/g	0.25	0.05	2.0
p_t		0.4	0.1	2.0

Table Appendix A.1: Parameter ranges, IVP model.
Empty unit means unitless parameter.

Parameter	Unit	Value	Min	Max
S_g	1/min	0.01	0.0	0.15
V_g	dl/kg	1.6	fixed	
p_{kabs}	g/min	1.6	1.0	5.0
p_{kt}	g/min	2.8	0.2	10
p_2	1/min	0.02	0.01	0.1
f		0.9	0.4	2.0
V_I	1/kg	0.06005	0.0	5.0
k_{cl}	1/min	0.16	0.0	1.0
k_d	1/min	0.0	0.0	0.1
S_I	l/(mU min)	0.009	0.0001	0.01
BW	kg	individually fixed		
G_b	mg/dl	96.8	68	120
I_b	mU/l	1.45	1.0	2.0
k_1	(dl mU)/mg	0.5	0.0	10
k_2	(dl mU)/(mg min)	0.015	0.0	10

Table Appendix A.2: Parameter ranges, SOGMM model.
Empty unit means unitless parameter.